

AN EXPERIMENTAL ANALYSIS OF GRAVITY-INDUCED FLOW
OF GRANULAR MATERIALS THROUGH
AN ANNULAR ORIFICE

By

VINCENT EUGENE SWEAT

Bachelor of Science in Agricultural Engineering

Kansas State University

Manhattan, Kansas

1964

Submitted to the faculty of the Graduate School of
the Oklahoma State University
in partial fulfillment of the requirements
for the degree of
MASTER OF SCIENCE
May, 1965

OKLAHOMA
STATE UNIVERSITY
LIBRARY

DEC 8 1965


AN EXPERIMENTAL ANALYSIS OF GRAVITY-INDUCED FLOW
OF GRANULAR MATERIALS THROUGH
AN ANNULAR ORIFICE

Thesis Approved:



Thesis Advisor





Dean of the Graduate School

593533

ACKNOWLEDGMENT

The writer wishes to express his sincere gratitude for the privilege of working under Dr. Gordon L. Nelson in this study. His guidance and assistance in carrying out the study and the preparation of this thesis are gratefully acknowledged.

A note of thanks goes to Mr. L. O. Roth for his assistance in photographic work.

The assistance of the Agricultural Engineering Department draftsmen in preparation of graphs and illustrations is appreciated.

The writer is indebted to Oklahoma State University and the Oklahoma Experiment Station for their financial support which made this study possible.

The staff of the Agricultural Engineering Department and the Agricultural Engineering Research Shop contributed valuable suggestions and encouragement throughout the study.

TABLE OF CONTENTS

Chapter	Page
I. INTRODUCTION	1
II. LITERATURE REVIEW	2
Introduction	2
Self-feeders	2
Flow Behavior of Granular Materials	3
III. THE STUDY AND EXPERIMENTAL DESIGN	11
Objectives	11
Pertinent Quantities	11
Formation of Pi Terms	14
Experimental Design	15
Assumptions and Limitations	19
IV. EXPERIMENTAL EQUIPMENT	20
Annular Orifice Assembly	20
Timer	23
Granular Materials	23
Flow Observation Device	25
V. PROCEDURE	27
Determination of Instantaneous Flow Rate	27
Determination of the Angle of Friction Between Material and Wall	28
VI. ANALYSIS OF DATA	29
Experiment 1	29
Adjustment of Experimental Design	31
Experiment 2	31
Experiment 3	33
Experiment 4	34
Experiment 5	36
Prediction Equations	39

Chapter	Page
VII. DISCUSSION OF RESULTS	41
Prediction Equations.	41
Comparison of Materials	43
Comparison With Previous Research	43
Flow in Model	46
Effect of Material Depth.	51
VIII. SUMMARY AND CONCLUSIONS	53
Suggestions for Further Investigation	55
SELECTED BIBLIOGRAPHY	56
APPENDIX A.	58
APPENDIX B.	60

LIST OF TABLES

Table	Page
I. Pertinent Quantities	12
II. Schedule of Experiments.	18
III. Properties of Granular Materials	24

LIST OF FIGURES

Figure	Page
1. Plot of Shear Stress Versus Compressive Stress.	6
2. Pressure Distribution Curves.	7
3. Definition Sketch of System	13
4. Grid Assembly	21
5. Grid Assembly With Cone and Gates	21
6. Complete Annular Orifice Assembly	22
7. Flow Observation Device	26
8. Experiment 1. Effect of H/D on GH/NeV^2	30
9. Experiment 2. Effect of x/d on NeV^2/Gx	32
10. Experiment 3. Effect of Outer Wall Slope on NeV^2/Gx	35
11. Experiment 4. Effect of Cone Slope on NeV^2/Gx	35
12. Experiment 4. Effect of Cone Slope θ on NeV^2/Gx	37
13. Experiment 5. Effect of ϕ' on Gx/NeV^2	37
14. Effect of Cone Slope Using Prediction Equation.	42
15. Effect of Outer Wall Slope Using Prediction Equation.	42
16. Effect of Orifice Width on Flow Velocity.	44
17. Effect of Outer Wall Slope on Flow Velocity	44
18. Effect of Cone Slope on Flow Velocity	45
19. Model Flow, $\alpha = 0^\circ$, $\theta = 30^\circ$	47
20. Model Flow, $\alpha = 0^\circ$, $\theta = 40^\circ$	47

Figure	Page
21. Model Flow, $\alpha = 0^\circ$, $\theta = 50^\circ$	48
22. Model Flow, $\alpha = -10^\circ$, $\theta = 30^\circ$	48
23. Model Flow, $\alpha = 5^\circ$, $\theta = 30^\circ$	49
24. Model Flow, $\alpha = 10^\circ$, $\theta = 30^\circ$	49
25. Model Flow, $\alpha = 20^\circ$, $\theta = 30^\circ$	50

CHAPTER I

INTRODUCTION

An increase in the mechanization of feed and grain handling has created a need for information concerning the flow of grain and feed materials through various types of orifices.

The use of self-feeders in feeding grain to livestock is dependent upon flow of feed through an orifice. Circular self-feeders utilize flow through an annular orifice. Applications of self-feeders are presently quite limited due to the inability of many feeds to flow in today's feeders.

In order to improve the operation of feeders and reduce their limitations, a more thorough and more applicable knowledge of the factors affecting flow of granular materials is required. Some information has been obtained from other areas of engineering concerning the flow of granular material, but biological materials present additional problems peculiar to the area of agricultural engineering.

CHAPTER II

LITERATURE REVIEW

Introduction

Some research has been done on the characteristics of flow of granular materials through orifices. Most of the previous work has been exploratory and qualitative in nature rather than quantitative due to difficulties encountered in attempting to measure flow properties of granular materials.

Self-feeders

The purpose of the first phase of the review of literature was to determine the position of self-feeders within the cattle industry. The importance of self-feeders and similar applications of orifice flow determine the need for orifice flow research within the agricultural industry.

The use of self-feeders for feeding grain to livestock offers several advantages in management. There is a saving in labor since feed is handled less often. An inexperienced feeder may successfully operate a feeding operation since many management decisions are eliminated. Less bunk space is required for a self-feeder system (3).

Recent feeding studies by Mochrie (20), Raun (25), and Carmody (6) indicate that cattle eat more and gain faster when self-fed.

Swift (27) investigated the proportions of daily feed energy used for body maintenance and that used for gain in weight in cattle. His study shows that the feed intake requirement for maintenance varies little with total feed intake. Thus, body gains are directly related to the amount of intake above that required for maintenance.

At Beltsville, Maryland, Putman and Davis (24) tested the feeding patterns of self-fed steers. These steers fed from 10 to 14 times daily with one-fourth of the total feeding time occurring at night between 6 p.m. and 6 a.m.

Cattle which are not used to grain cannot be self-fed on a grain-only ration until they are brought to full feed. Morrison (22) cites the practice of mixing chopped hay with grain to start cattle on a self-feeder. Cotton hulls or other types of bulk material may also be mixed with grain for a starter ration.

Four types of self-feeders were observed in a study by the author. Self-feeders observed tended to bridge over above the outlet for more difficult flowing materials. Plug flow generally occurred with straight-sided feeders. This caused some segregation of fine and coarse particles.

Wastage was excessive in three of the feeders which all had spacious troughs with horizontal bottoms. Large amounts of feed accumulated in the troughs, allowing segregation of different particle sizes and aging and wastage of feed. The feeder which had a trough with a sloping bottom had no segregation of particles and very little wastage.

Flow Behavior of Granular Material

Gravity-induced flow of granular material depends upon the strength characteristics of the mass of particles. High strength characteristics

allow rigid structures such as domes and pipes to form in the mass. These structures halt flow (12).

Brown and Hawksley (5) describe free flow of granular materials as similar to flow occurring in a stationary granular mass when subjected to shearing forces in that particles tend to move in groups. The method of formation of these groups and their density is not known. The boundaries between groups are clearly defined and resemble lines of slip (5). Flow is irregular and asymmetrical. There is a similarity of flow patterns between gravity-induced flow through an orifice and a turbulent jet of fluid moving in the opposite direction (5).

Several factors affect the flow of granular materials. Jenike (12) found that ability of a granular mass to flow decreases with time and also decreases with an increase in density.

Strength of a granular mass increases as the compacting pressure increases. Lower compacting pressures produce better flow (11). Pressure breakers which consist of horizontal, load-carrying devices reduce the pressure at the outlet and promote better flow (11).

The ability to flow of a solid containing a range of particle sizes is governed by the flow properties of the fine fraction since shearing takes place across the fines during flow (12). The size of the coarse particles will affect flow as particles tend to interlock at the outlet.

One of the biggest problems in analyzing the flow of granular materials is defining and measuring the physical properties of the material. Kondner and Green (14) described the physical properties of sand in a dimensional analysis study of the lateral stability of poles in sand. The quantities used to describe the deformation characteristics

of the sand were its dry density, angle of internal friction, and "viscosity." The units describing viscosity were force x time /distance². Viscosity referred to the time dependent deformation characteristics observed in the experiment.

One of the dimensionless terms used was dct/v .

d = dry specific weight

t = time of loading

c = perimeter of pole

v = viscosity.

The term, dct/v , was considered to be the ratio of the time of loading to a relaxation time of the soil. In soil tests it varied but had little effect.

In a study of load bearing capacity of soils, Kondner and Krizek (15) attempted to describe strength characteristics of the soil with these three parameters:

q = strength parameter of a soil $\dot{=} FL^{-2}$

v = viscosity of soil $\dot{=} FL^{-2}T$

ϕ = angle of internal friction.

Creep and viscous effects were given by $qt/v + Ft/Av$, where F is force; A is the area; and t is the time of loading. Lack of information on strength characteristics prevented development of a prediction equation.

A loose, unconfined, bulk material has no shear, compressive, or tensile strength, but the same material under compacting pressures exhibits resistance to compressive, tensile, and shearing forces. The amount of compressive strength built up under a compacting pressure will govern the ability of a material to flow (12). To describe the

ability of a material to flow, Jenike (12) introduced the flow-factor,

$$f_c/2 = F(v/w),$$

where f_c is the unconfined compressive strength of material under a given compacting pressure, v . Unconfined compressive strength is defined as the load per unit area at which unconfined prismatic or cylindrical samples of material fail in a simple compression test. w is the unit weight of the material.

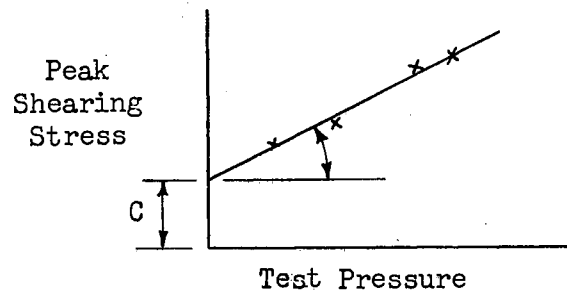


Figure 1. Plot of Shear Stress Versus Compressive Stress.

A transverse shear test machine was used to measure f_c/w .

$$f_c = 2c \tan (45^\circ + \phi/2)$$

c = cohesion

ϕ = angle of internal friction = slope of line obtained where peak shearing stress is plotted as the ordinate and test pressure as the abscissa, as in figure 1.

Lee (17) applied Janssen's formula for finding bin pressures to a conical bottomed hopper and obtained pressure distributions similar to those found by Jenike. These are shown in Figure 2. A different pressure distribution curve was plotted for each depth. Each curve

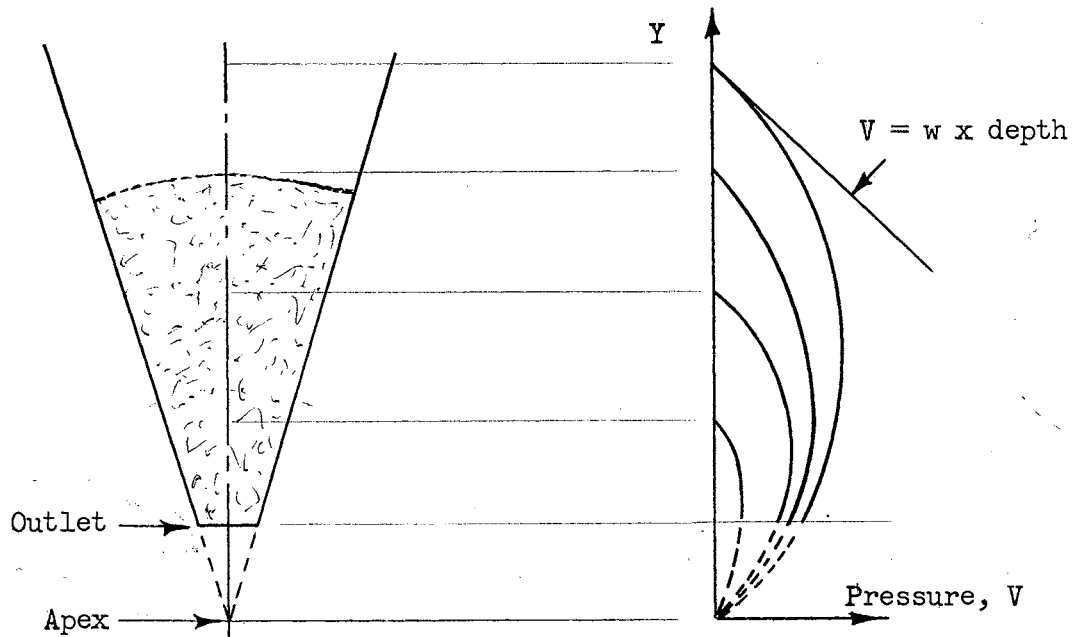


Figure 2. Pressure Distribution Curves.

starts at the top as a tangent to the hydrostatic line and returns to zero where the apex of the hopper would be. The maximum pressure occurs at a height slightly below the center of the hopper (17).

Endersby suggested that resistance to deformation in a granular material is caused by internal friction and "structural resistance". The internal friction was found by experiment to be independent of the void ratio of the initial packing. The structural resistance varied with the size of the test specimen. (A triaxial test was used with the results obtained by plotting a Mohr diagram.) Structural resistance was found to be dependent on density and maximum particle size and independent of the addition of fine particles (5). The fines may present resistance to rolling similar to the action of grit in a bearing.

A dimensional analysis approach was used by Fowler and Glastonbury (8) who performed tests on sugar, sand, rape seed, wheat, and rice to determine the factors affecting flow of these granular materials through circular orifices. The following equation was developed:

$$\frac{W}{bA(2gD_h)^{0.5}} = 0.236 (D_h/sd)^{0.185} \quad (2.1)$$

W is the pounds mass discharged per second, b is the bulk mass density of the solids, A is the flow area of the orifice of hydraulic diameter, D_h , d is the average arithmetic screen diameter used in sizing the particles, g is the gravitational acceleration, and s is the average shape factor of the particles. The effect of head and container diameter were found to be insignificant in this particular analysis. Flow rate was influenced by a ratio of orifice diameter to particle diameter less than 5. The coefficient of friction was characterized with fundamental factors of particle shape and diameter, and surface roughness. (8).

Experiments to determine the variables affecting the angle of friction of dry granular materials were conducted by Fowler and Chodziesner (9). Their results showed that the angle of friction of solids sliding on surfaces depends on the shape factor, specific gravity, and diameter of the material and on the roughness of the surface of the wall.

Beverloo, Leniger, and van de Velde (4) investigated flow of seeds through various orifices. Three copper cylinders having a height of 30 cm. and internal diameters of 5, 10, and 15 cm. were used. Each cylinder had a flat bottom which could be fitted with various sizes and shapes of orifices. Materials used included sand, linseed, spinach,

watercress, rapeseed, kale, and swede. For circular orifices flow velocity, V , was expressed as a function of the orifice diameter, D_o , and the average particle size, d ; $V = C(D_o - kd)^{2.5}$. C is a coefficient containing the bulk density and the gravitational constant. k is a dimensionless coefficient with a value of approximately 1.4 for all seeds used. It was not correlated with the angle of repose but was thought to be a function of particle surface properties. $(D_o - kd)$ is the effective orifice diameter and is affected by the particle size. Effective diameter was used because flow did not occur within a narrow ring of area at the edge of the orifice.

In tests conducted by Laforge and Boruff (16), surface roughness influenced flow velocity. A symmetrical hopper with a square orifice was used with and without a coating of coarse sandpaper. For slopes less than 45-50°, rough surfaces yielded higher flow velocities of cohesionless granular materials. For steeper slopes, the smooth surface produced the highest velocities. No explanation was given concerning the differences in flow between the smooth and rough surfaces.

Laforge and Boruff (16) also varied the slopes of the pyramid-shaped hopper. Flow velocity was a minimum between 20° and 40° slopes. It was nearly the same for a flat bottom (slope equals 0°) and a slope of 50°, with a sharp increase above 50°. Their results indicate that increasing the slope of the hopper walls above 0° increases lateral particle momentum which restricts and retards the main vertical flow column and reduces flow velocity. As the angles increase above 45°, the restrictive influence of lateral momentum is offset by the vertical

momentum of particles moving along the sloping walls. These investigators also state that the influences of slope and surface roughness are contained within a one-inch band adjacent to the orifice; the effect of the rest of the hopper is small.

CHAPTER III

THE STUDY AND EXPERIMENTAL DESIGN

Objectives

The objectives of the study were as follows:

1. Determine the factors which affect vertical, gravity-induced flow of granular material through an annular orifice.
2. Determine the effect of the above factors on vertical, gravity-induced flow of granular material through an annular orifice.
3. Develop information useful for the design of self-feeders which utilize flow through an annular orifice.

The factors studied were those pertaining to the physical properties and configuration of a feeder utilizing an annular orifice. The specific granular materials used in the study were livestock feed materials.

Pertinent Quantities

A dimensional analysis was used in this study. One of the first steps in a dimensional analysis is to identify and list the pertinent quantities, or those quantities which are known to have or are considered to have significant effect on the problem.

Those quantities which were considered to influence gravity-induced flow of granular materials through an annular orifice are listed in Table I.

The gravitational constant, G , determines the weight of the material.
 Newton's coefficient, N_e , relates inertial force and mass in the system.
 H , the depth of material above the orifice affects the internal

TABLE I
 PERTINENT QUANTITIES

No.	Symbol	Description	Units	Dimensional Symbol
1	G	Gravitational Field Strength	Lb_f/Lb_m	FM^{-1}
2	N_e	Newton's Second Law Coefficient	$\frac{Lb_f - Sec^2}{Lb_m - Ft}$	$FM^{-1}L^{-1}T^2$
3	H	Depth of Material Above Orifice	Ft	L
4	x	Width of Orifice	Ft	L
5	D	Bottom Diameter of Cone	Ft	L
6	d	Average Particle Diameter	Ft	L
7	ρ_B	Bulk Mass Density	Lb_m/Ft^3	ML^{-3}
8	E_t	Stiffness Index of Walls	Lb_f/Ft	FL^{-1}
9	V	Instantaneous Volume Flow Rate Per Unit Area Through Orifice	Ft/Sec	LT^{-1}
10	ϕ'	Angle of Friction Between Material and Metal Surfaces	Degrees	----
11	ϕ	Internal Angle of Friction of Material	Degrees	----
12	θ	Slope of Cone	Degrees	----
13	α	Slope of Outer Wall	Degrees	----
14	v	Voids Ratio of Material	----	----

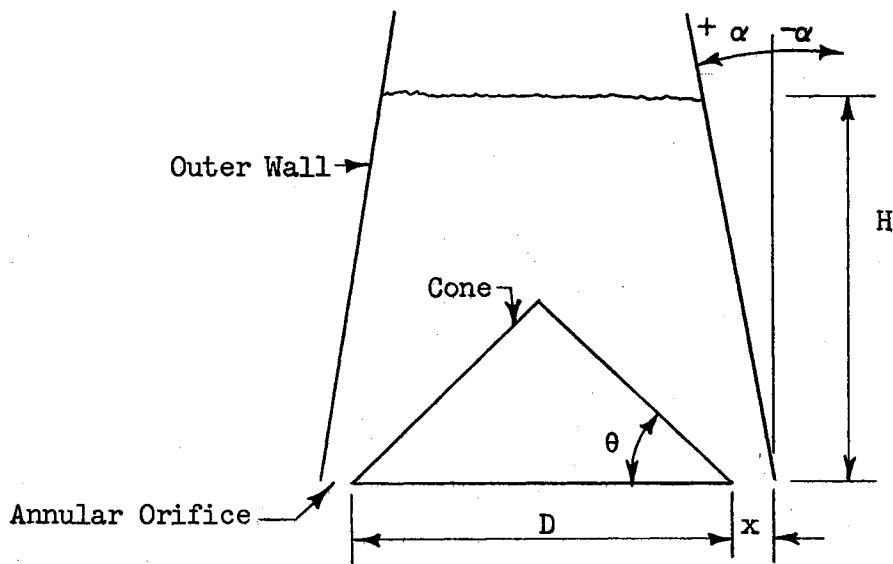


Figure 3. Definition Sketch of System.

pressure of the granular mass was considered to be a possible influencing factor.

D was the bottom diameter of the cone. The width of the orifice was x .

The average particle size, d , was listed as a pertinent quantity. The maximum particle size is known to have an influence on flow for small orifice widths. Flow cannot occur when the maximum particle size is greater than the orifice width. The average particle size was considered to give a more adequate description of particle size.

The slope of the cone, θ , and the slope of the outer wall, α , were believed to have an effect on flow. Previous research with symmetrical hoppers shows that the slope of walls adjacent to an orifice affects flow.

The bulk mass density, ρ_B , of the granular material determines the weight of granular material within a given volume of the feeder.

It is the stiffness index of the wall and cone material and has been found to affect the pressures in a bin so it is included in the list of pertinent quantities. E is the modulus of elasticity of the wall and cone material and t is the thickness of the wall and cone material.

V is the instantaneous volume flow rate per unit area through the orifice.

The angle of friction between the feed and the outer wall, ϕ' , affects the resisting force exerted by the wall in a direction parallel to the wall. ϕ , the internal angle of friction of the material affects the resisting force exerted by a stationary wall of the material. It also determines the shear forces necessary to initiate flow.

The voids ratio, v , relates bulk density and the particle density of the granules.

Formation of Pi Terms

There were fourteen pertinent quantities which were described in four dimensions. By the Buckingham Pi Theorem there must be ten dimensionless terms to describe the system. These ten independent, dimensionless terms may be derived from dimensional analysis theory. There is a large number of groups of ten dimensionless terms which would satisfy the theoretical requirements. However, formation of the groups in this manner does not insure that each term is physically meaningful.

The following terms were formed by inspection and were proved to be independent by use of matrix theory:

$$\begin{array}{lll} \pi_1 = \frac{GH}{NeV} 2 & \pi_5 = \theta & \pi_8 = X/D \\ \pi_2 = H/D & \pi_6 = \phi' & \pi_9 = \nu \\ \pi_3 = x/d & \pi_7 = \phi & \pi_{10} = \rho_B \frac{GD^2}{Et} \\ \pi_4 = \alpha & & \end{array}$$

π_1 was expressed as a function of the other pi terms.

$$\pi_1 = f(\pi_2, \pi_3, \pi_4, \pi_5, \pi_6, \pi_7, \pi_8, \pi_9, \pi_{10}) \quad (3.1)$$

Experimental Design.

It was not possible to determine the effect of all the dimensionless terms in the time available for this study. For this reason the effects of four of the dimensionless terms were not studied. ϕ , ν , and $\rho_B GD^2/Et$ were held constant. These three terms were considered to have a possible effect on the flow studies but this effect was not determined.

x/D was not held constant. It was believed that changes in x/D may cause variations in flow between extreme values of x/D , but it was not considered to cause significant variation in the narrow range of values (0.0194 - 0.0689) which it assumed in this study. Tests performed by Fowler and Glastonbury (8) showed that a similar parameter had no effect on flow through a circular orifice.

$\pi_{10} = \rho_B GD^2/Et$ remained at a constant value throughout the experiment. The cone bottom diameter, D , was constant for all cones. Et was constant since all cones and outer walls were made of the same material. The bulk mass density, ρ_B , was constant as the same material

was used throughout each experiment and the test hopper was filled from an overhead hopper in the same manner for each observation. This also insured a constant value of v and ϕ . The materials were kept in air-tight containers to prevent moisture losses in a further effort to maintain constant physical properties of the material.

Other possible variations in ρ_B were considered insignificant. Volumetric expansion due to temperature changes was disregarded since only large temperature changes could significantly change the bulk density of the material. During the period in which the experiments were conducted the temperature of the granular materials and the cones and outer walls did not vary over a large range. Density increases due to long durations of time after filling the test hopper were eliminated by making all test observations within three minutes after filling the hopper.

Elimination of four pi terms reduces equation 1 to this expression:

$$\pi_1 = f(\pi_2, \pi_3, \pi_4, \pi_5, \pi_6) \quad (3.2)$$

This function can be determined from experimental data.

The method for determining a prediction equation for π_1 as a function of the other pi terms is as follows. (1) Vary the first independent pi term while holding the other pi terms constant. Then develop a component equation for π_1 as a function of this pi term. (2) Vary the other independent pi terms one at a time and develop a component equation for π_1 as a function of each of the remaining pi terms. (3) Combine the component equations into one prediction equation.

Following is a discussion of the pi terms in equation 3.2. The dependent pi term is $\pi_1 = GH/NeV^2$. This term was evaluated in each experiment as a function of one of the independent terms.

$\pi_2 = H/D$ depended upon the geometry of the test hopper. This quantity assumed six different values from 1.882 to 0.775, achieved by changing H.

Values of $\pi_3 = x/d$ ranged from 2.756 to 9.803 for milo, from 7.292 to 25.94 for material D, and from 8.537 to 30.37 for material B. The value of d was constant for each material. The orifice width, x, varied from 0.35 inches to 1.25 inches.

$\pi_4 = \alpha$ is the slope of the outer wall and was measured according to the definition sketch on page 13. The values used were -10° , 0° , 5° , 10° , and 20° . Values outside this range might have given a more complete picture of the complete function of π_1 versus α but were not considered to be within the range of values used in practical applications of feeders.

$\pi_5 = \theta$ is the slope of the cone. Separate cones were used for each value of θ . Values of θ were 0° , 15° , 30° , 40° , 45° , 50° , 55° , 60° , and 65° .

$\pi_6 = \phi'$ is the angle of friction between the granular material and the cones and outer walls. By using different coatings on the galvanized steel, values from 10° to 30° were obtained.

In the analysis of data the tangents of the angles α , θ , and ϕ' were used.

Table II shows the schedule of experiments which were conducted in the analysis. Because of the differences between materials, values of π_1 , π_3 , and π_6 were different for each material. Values of π_2 , π_4 , and π_5 were the same for each material.

SCHEDULE OF EXPERIMENTS

Experiment	$\pi_1 = \frac{C\alpha}{2 \text{ NeV}}$	$\pi_2 = \frac{H}{D}$	$\pi_3 = \frac{x}{d}$			$\pi_4 = \tan \alpha$	$\pi_5 = \tan \theta$	$\pi_6 = \tan \phi'$			
			Milo	D	B			Milo	D	B	
1	Measure	0.775	5.791	15.312	17.927	0.0000	.5774	0.1944	0.1780	0.1944	
		0.996									
		1.217									
		1.439									
		1.660									
		1.882									
2	Measure	1.882	2.756	7.292	8.537	0.0000	.5774	0.1944	0.1780	0.1944	
			3.543	9.375	10.976						
			5.791	15.312	17.927						
			7.677	20.313	23.780						
			9.803	25.938	30.366						
3	Measure	1.217	3.543	9.375	10.976	0.0000	.5774	0.1944	0.1780	0.1944	
											0.3640
											0.1763
											0.0875
											0.0000
	-0.1763										
4	Measure	1.217	3.543	9.375	10.976	0.0000	0.0000	0.1944	0.1780	0.1944	
							0.2679				
							0.5774				
							0.8391				
							1.0000				
							1.1918				
							1.4281				
							1.7321				
							2.1445				
5	Measure	1.217	3.543	9.375	10.976	0.0000	.5774	0.1944	0.1780	0.1944	
								0.2309	0.2868	0.2680	
								0.3640	0.5095	0.4663	
								0.5317	0.5774	0.6009	

Assumptions and Limitations

Because of the lack of a simple and accurate method of describing the flow properties of a specific granular material, only three materials were used in the study and a separate analysis was made for each material. It was assumed that all pertinent physical properties of the materials used remained constant throughout the experiment.

CHAPTER IV

EXPERIMENTAL EQUIPMENT

Annular Orifice Assembly

Pictures of the annular orifice assembly are shown in Figures 4, 5, and 6.

The outer walls and cones were made from 24 gage galvanized steel sheet. One adjustable vertical outer wall was made with 6 columns of holes in one end which provided variation in diameter from $18\frac{1}{2}$ to $20\frac{1}{2}$ inches. Four outer walls were cone frustums as shown in Figure 6. Two frustums had a slope of 10 degrees; one had a base diameter of 19 inches and the other had a top diameter of 19 inches. The other two frustums were 19 inches in diameter at the base and had slopes of 85 degrees and 70 degrees, respectively.

Nine cones were made, each having a base diameter of 18 inches. The apex angles varied from 50 to 150 degrees. One flat sheet was used. The bottoms of the cones were stiffened with a $\frac{1}{4}$ inch diameter iron hoop welded on the inside.

The outer walls and cones were supported by a grid shown in Figure 4.

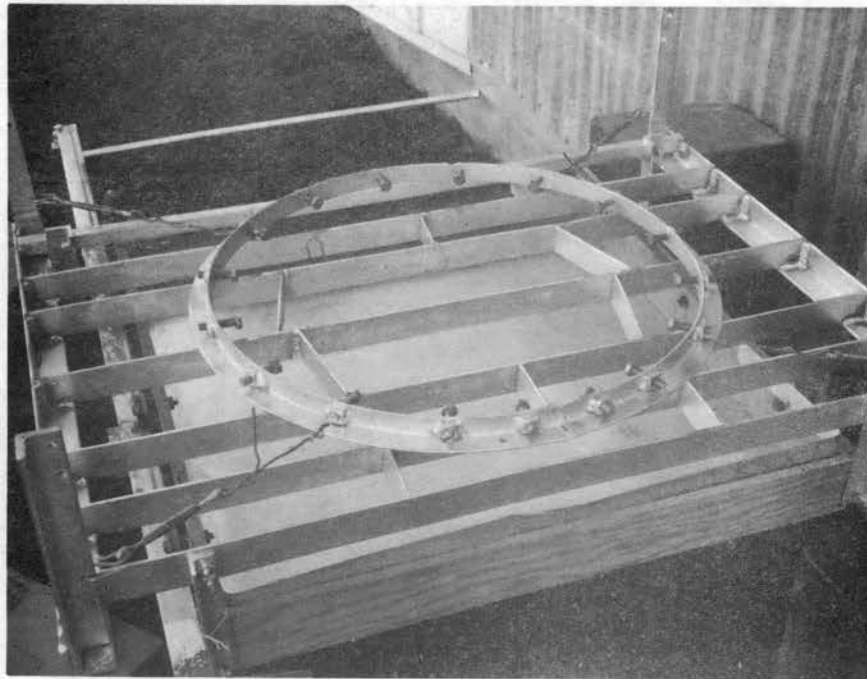


Figure 4. Grid Assembly.



Figure 5. Grid Assembly With Cone and Gates.

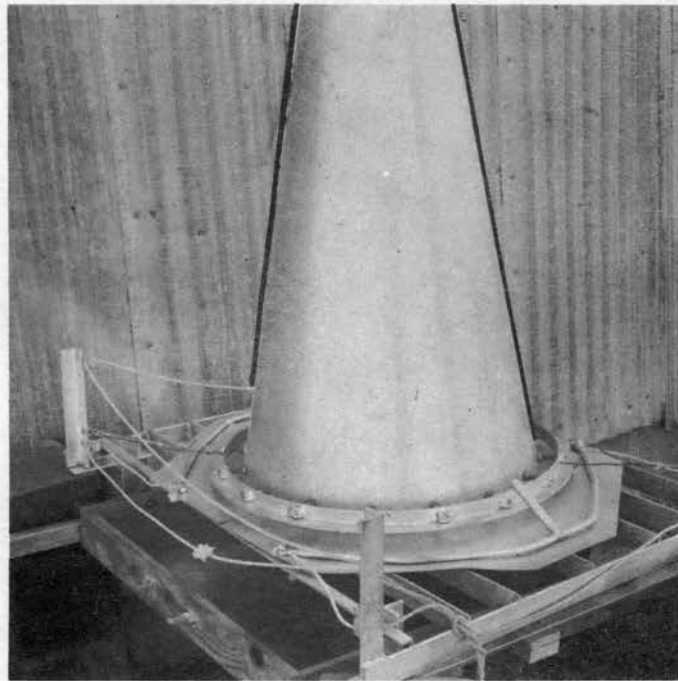


Figure 6. Complete Annular Orifice Assembly.

It consisted of $1/8$ " by $1-1/2$ " steel straps oriented vertically and fastened at the ends to angle irons. The spacing of the grid members was such that the cone made contact with the grid at six equally spaced points. The tops of the vertical straps were filed to a point in the area where flow occurred to minimize reduction in flow area due to the grid.

Two hemispherical gates were used to close the flow area. These gates were positioned against the bottom of the cone and were directly below the outer wall. The gates were opened simultaneously with a rope and pulley system. Figure 5 shows the catch box beneath the cone in position to catch material.

A circular $1-1/8$ " angle iron with 16 bolts tapped into it was used to position the outer walls and maintain an orifice opening of uniform width. The bolt heads were tightened against the outer wall pictured in Figure 6. The ring was held in place by a supporting system consisting of four turnbuckles fastened to the ring and to the corners of the grid frame.

Timer

An electric timer was used to measure the length of time that the catch box was under the orifice during the test. The timer was actuated with a switch placed below the grid. The switch was actuated by the catch box as it was moved in and out from under the grid.

Granular Materials

Three granular materials were used. These were grain sorghum and two feed rations consisting primarily of steam rolled grain sorghum.

A seive analysis as officially recommended by the American Society of Agricultural Engineers (19) was performed on each material. A Modulus of Uniformity and a Fineness Modulus were found for each material. The average particle size was determined from the same seive analysis.

The following table lists the properties of the granular materials which were used.

TABLE III
PROPERTIES OF GRANULAR MATERIALS

Property	Milo	Ration D	Ration B
Fineness Modulus	4.96	3.55	3.33
Modulus of Uniformity (Coarse, Medium, Fine)	9½:½:0	1:7½:1½	1:7:2
Average Particle Size, Inches	0.127	0.048	0.041
Percent Moisture, (dry basis)	7	8	8
Bulk Density, lb _{mass} /ft. ³	47.7	39.7	39.1

Rations B and D contained 84½% steam rolled milo, 8% cottonseed meal, 5% dehydrated alfalfa meal, 3% molasses, and 1½% urea. Ration D had stabilized animal tallow added to it amounting to 5% of the total weight.

Each material was run through a 5 mesh screen to remove lumps and trash.

Flow Observation Device

When the cone angle and the outer wall angle were varied the data obtained did not assume a smooth curve. In an attempt to explain these apparent discontinuities in flow, a glass-sided model was made with a cross section similar to the cross section of the annular orifice assembly used in the experiments so that flow patterns for various slopes could be observed.

A sketch of the flow observation device is shown in Figure 7. The "cone," "outer wall," and adjustable walls were made of flat galvanized sheet material. The cross members connecting the plexiglass front and plywood back were 10 inches long. Positioning rods inserted through holes in the front and back held the "cone" and "outer wall" at any specified angle. The "cone" and "outer wall" were welded to pivot rods which extended through holes in the front and back. The opening between the pivot rods was $\frac{1}{2}$ inch wide.

A gate was placed beneath the opening when the hopper was filled. Then the gate was removed and flow was observed. Pictures were taken of the flow using a shutter speed of $\frac{1}{5}$ second so that the moving seeds were blurred showing the flow patterns existing in the cross section. Seven of these pictures are shown in Figures 17-23.

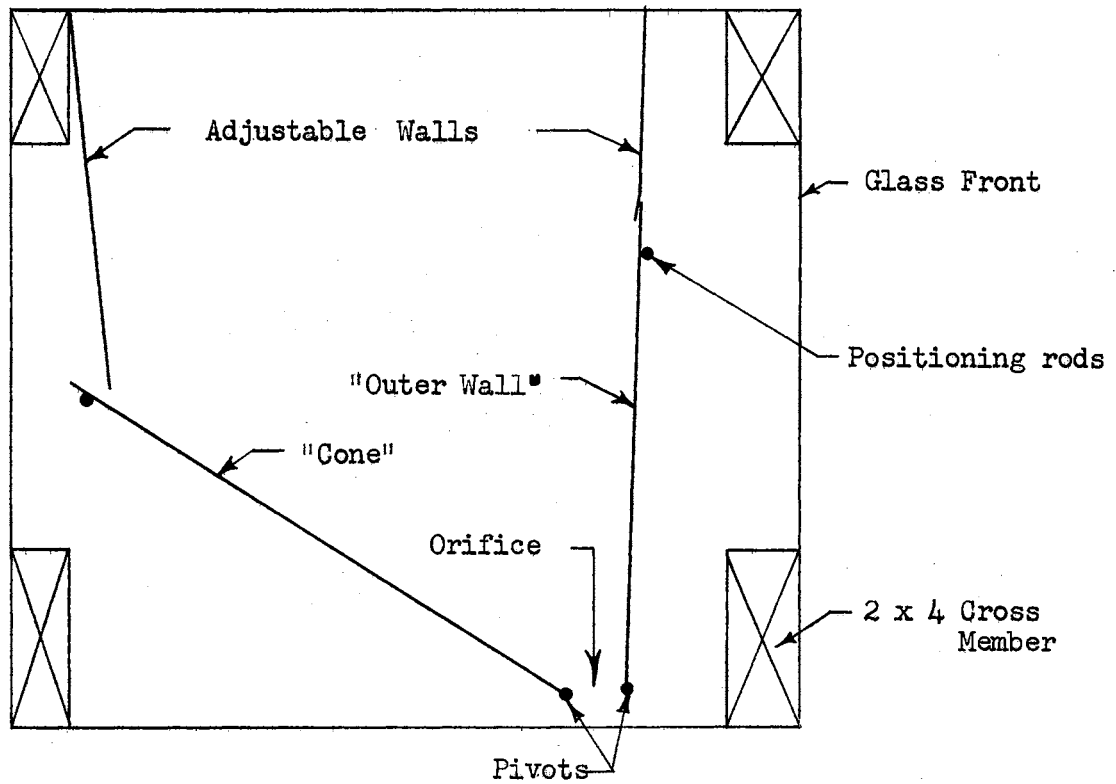


Figure 7. Flow Observation Device.

CHAPTER V

PROCEDURE

Determination of Instantaneous Flow Rate

The test hopper was filled to the appropriate depth from a hopper placed directly above it to insure uniform filling. The top surface of the granular material in the test hopper was leveled.

The gates around the edge of the cone were opened. Immediately after flow was established, the catch box was rolled under the feeder for one to three seconds and pulled out.

The forward edge of the catch box actuated a timer switch as it passed directly under the center of the cone on both passes in and out. The time that the catch box was under the orifice was measured by an electric timer which allowed readings to the nearest 0.0001 of a minute. The material caught in the catch box was weighed on a balance type scale.

The test hopper was emptied completely during each test. Fourteen cans one foot in diameter were used to catch the material and transfer it to the hopper above the test hopper. To avoid cracking the material no mechanical conveyors were used.

Five successive replications were made of each test.

The initial depth was greater than H to compensate for the material which flowed out before the catch box was rolled under the orifice.

H was considered to be the average depth of material during the short interval when flow was being caught.

Determination of the Angle of Friction
Between Material and Wall

A sample of the cone and outer wall material was placed on a tilting table surface. A sample of granular material was placed in an inverted bottomless tray on top of the wall material in such a manner that the tray did not touch the wall material. The tilting table surface was tilted slowly until the tray started sliding. The angle at which sliding started was recorded as the angle of friction between the granular material and the wall material.

The sample cone and outer wall material were coated or treated in the same manner as the cone and outer wall of the test hopper. ϕ' was measured at the time of testing. The galvanized steel sheet material was polished with fine steel wool to obtain low values of ϕ' . Paint and lacquer coatings were applied to produce higher values of ϕ' .

CHAPTER VI

ANALYSIS OF DATA

Experiment 1

H/D was varied in Experiment 1. The mean of five replications at each value of H/D was plotted in Figure 8.

A linear regression analysis was applied to the logarithms of GH/NeV^2 and H/D for each material. The form of the regression equation is $\ln(GH/NeV^2) = A + b(\ln H/D)$. It was hypothesized that the slope (b) of the regression line for each material was not significantly different from 1.0. If $b = 1.0$ and $A = 0.0$, then $GH/NeV^2 = H/D$. Dividing both sides of the equation by H eliminates H from the expression. Then H does not affect flow velocity and may be deleted from the list of parameters affecting orifice flow.

The values of b and the 90% confidence interval for b as determined by the statistical analysis are:

$$\text{Milo} - b = 1.0235 \pm 0.03648; \quad 0.9888 < b < 1.0618$$

$$D - b = 1.0010 \pm 0.03713; \quad 0.9639 < b < 1.0382$$

$$B - b = 1.0884 \pm 0.03056; \quad 1.0579 < b < 1.1200$$

The hypothesis that $b = 1.0$ is true for milo and material D.

However the slope of the regression line for material B is significantly different from 1.0.

The following comparison was performed to determine the significance of this difference in slope: When $b = 1.0$ the predicted difference between $\ln GH/NeV^2$ (maximum) and $\ln GH/NeV^2$ (minimum) is equal to the slope b multiplied by $(H/D_{max} - H/D_{min})$. This is $1.0 \times (3.834 - 2.947)$. But $b = 1.0884$ so the predicted difference between the same two values is $1.0884(H/D_{max} - H/D_{min}) = 1.0884 (3.834 - 2.947) = 0.967$. The difference between these two predicted values of GH/NeV^2 is the error introduced by assuming that $b = 1.0$. It is equal to $(0.967 - 0.887)(\ln GH/NeV^2_{ave.}) = 0.080/4.22 = 1.9\%$.

Since this error was so small, the hypothesis, that the slope (b) of the linear regression line for material B is 1.0, was accepted.

H was not considered to have an important effect on flow velocity for the observed range of H/D in this experiment.

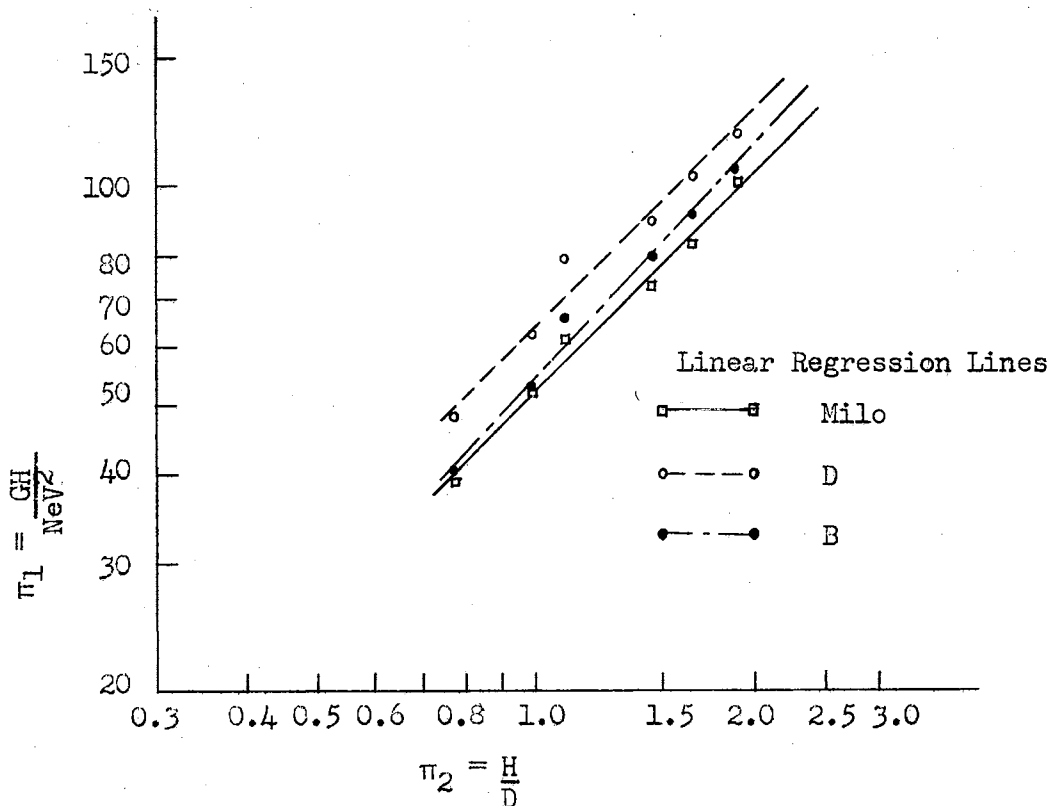


Figure 8. Experiment 1. Effect of H/D on GH/NeV^2 .

Adjustment of Experimental Design

Since the foregoing analysis revealed that H was not pertinent, $\pi_2 = H/D$ was deleted from the group of π terms. $\pi_1 = GH/NeV^2$ also contained H . This H was replaced by the orifice width, x , to make the remaining data analysis more meaningful. Then $\pi_1 = Gx/NeV^2$ and the nine π terms which remained after H/D was deleted were still independent.

The adjusted experimental design was the same as in Table II with these changes: Experiment 1 was deleted. The column containing $\pi_2 = H/D$ was deleted. $\pi_1 = Gx/NeV^2$.

Experiment 2

In Experiment 2, x/d was varied. The observed values of NeV^2/Gx for each material were plotted in Figure 9. Each point represents the mean of five replications.

As x/d increased, NeV^2/Gx approached a constant value. Observation of the data indicated that NeV^2/Gx had approached a constant value for materials B and D but not for milo.

A linear regression analysis was performed on the data for materials B and D. The lowest value of x/d for material B was not included since NeV^2/Gx did not appear to have approached a constant value at that point. A "t" test ($t = b/\text{standard deviation of } b$) was used to show that the slopes (b) of the regression lines for B and D were not significantly different from zero at the 90% confidence level. These regression lines are shown in Figure 9.

NeV^2/Gx for milo appeared to approach a constant value slightly beyond the range of values of x/d used. The data was fitted to a function of the form

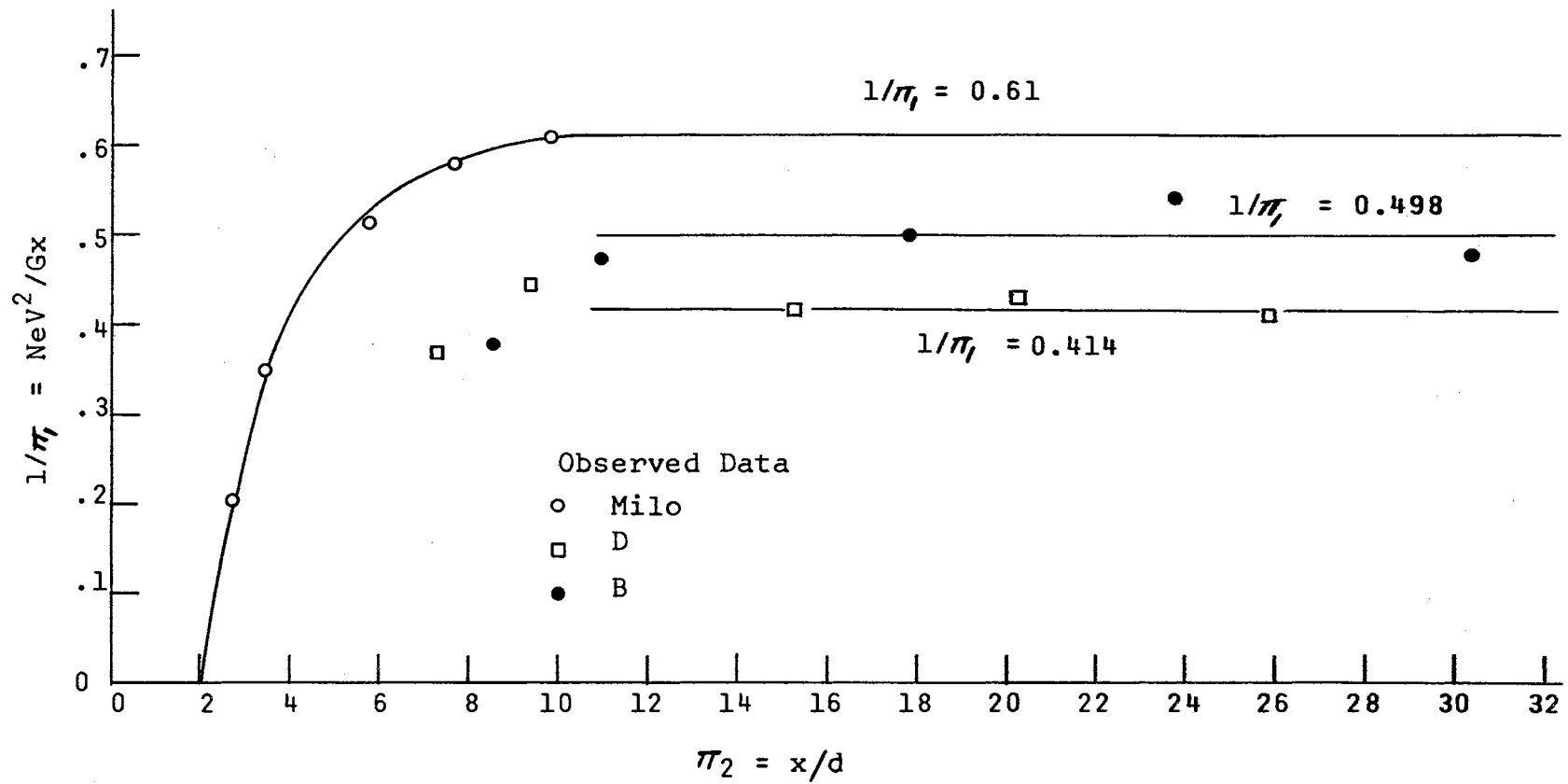


Figure 9. Experiment 2. Effect of x/d on NeV^2/Gx .

$$\text{NeV}^2/\text{Gx} = C_1(1 - e^{-C_2(x/d - C_3)})$$
 which is similar in form to the plotted response curve which was obtained. C_1 is the constant value approached by NeV^2/Gx as x/d exceeds 12. C_3 is the value of x/d for which NeV^2/Gx approaches zero. This curve does not go through the origin since flow ceases when the average particle size, d , approaches one half the magnitude of the orifice width. A computer program was used to find the values of the constants which gave the best fit to the data. $C_1 = 0.61$, $C_2 = 0.54$, and $C_3 = 2.0$.

NeV^2/Gx approached constant values of 0.414 and 0.498 for D and B, respectively. The range of x/d was not low enough to determine exactly where the limiting value of NeV^2/Gx was reached for B and D.

For x/d greater than 12, NeV^2/Gx is constant for each material. $\text{NeV}^2/\text{Gx} = C_1$. Then $V^2 = C_2x$, or $V = C_3(x)^{\frac{1}{2}}$.

The component equations for each material for x/d greater than 12 are: NeV^2/Gx (milo) = 0.61; NeV^2 (D) = 0.414; and NeV^2 (B) = 0.498. These equations do not apply where x/d is less than 12.

Experiment 3

The slope of the outer wall, α , was varied in Experiment 3. There were five different values of α for milo and four for materials D and B.

The hypothetical form of the function relating NeV^2/Gx to $\tan \alpha$ was assumed to be parabolic as shown in Figure 10 for the following reasons. As α approaches (90° - material angle of repose), the flow should approach a constant value since α has no effect when the slope of the outer wall is below the material angle of repose. The maximum flow velocity was hypothesized to be near $\alpha = 0^\circ$. A parabolic function satisfies these conditions and is convenient to use.

The experimental data assumed a parabolic distribution with the exception of the point $\alpha = 5^\circ$. Flow of each material was at least 20% slower at this observation than for adjacent values of α . A complete replication of this particular experiment produced nearly identical results.

A parabolic curve was fitted to the data for possible use as a component equation. This equation does not predict variation in NeV^2/Gx for values of α near 0° .

In a further attempt to explain the apparent discontinuity in the observed data, pictures were taken of flow in a cross-sectional model of the test hopper. The analysis of these pictures is presented in the "Discussion and Results."

The component equations for Experiment 3 are:

$$\text{Milo} - \text{Gx}/\text{NeV}^2 = 2.754 - 2.807 \tan \alpha + 8.996 \tan^2 \alpha \quad (6.1)$$

$$\text{D} - \text{Gx}/\text{NeV}^2 = 2.494 - 1.629 \tan \alpha + 11.58 \tan^2 \alpha \quad (6.2)$$

$$\text{B} - \text{Gx}/\text{NeV}^2 = 2.050 - 1.448 \tan \alpha + 7.300 \tan^2 \alpha \quad (6.3)$$

Experiment 4

The pi term varied in Experiment 4 was θ , the slope of the cone. The observed data is plotted in Figures 11 and 12.

The form of the response curve for varying $\tan \theta$ was hypothesized to be as shown in Figure 11. NeV^2/Gx will approach a constant value for θ below the material angle of repose since the flow was not affected by θ in this region. It was also hypothesized that NeV^2/Gx would approach a constant value as θ approached 90° when α is 0° . No attempt was made to fit the data to this type of curve.

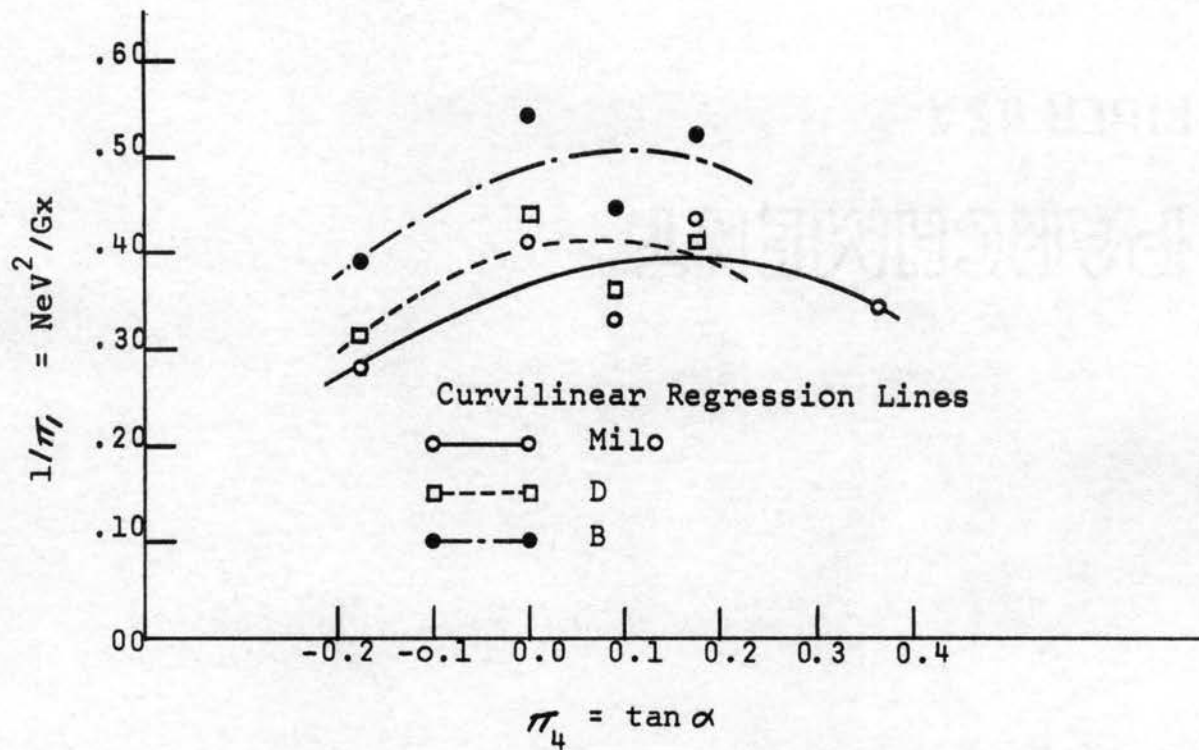


Figure 10. Experiment 3. Effect of Outer Wall Slope on NeV^2/Gx .

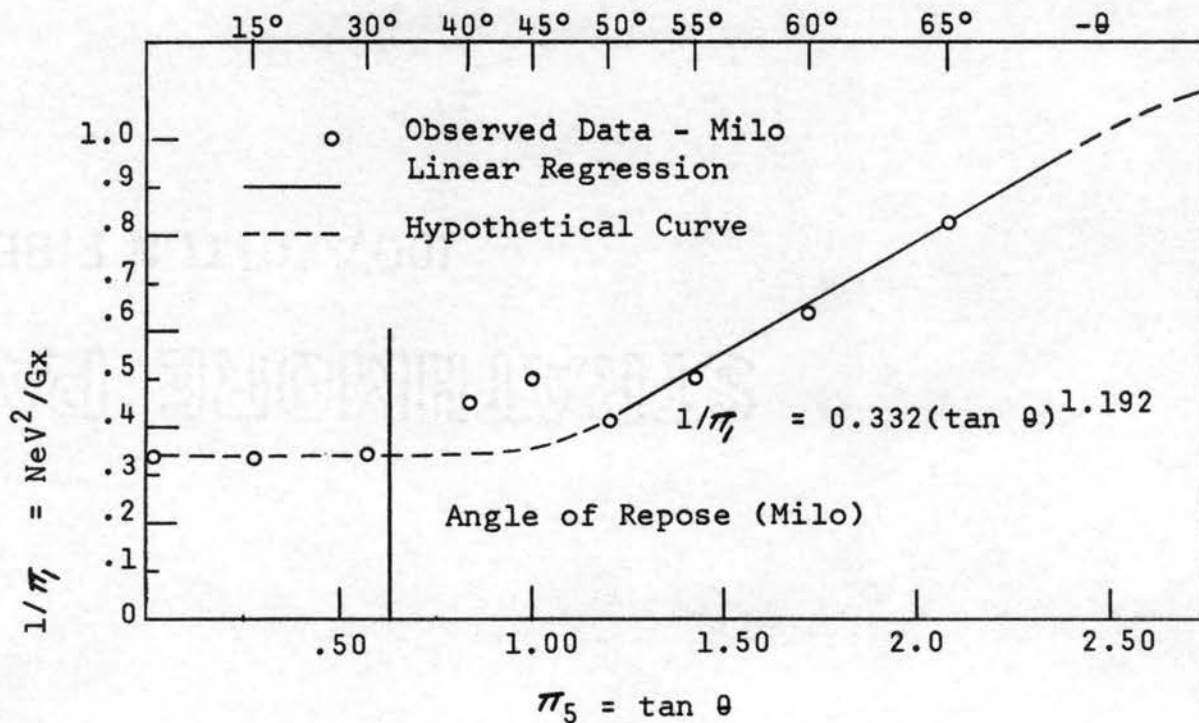


Figure 11. Experiment 4. Effect of Cone Slope on NeV^2/Gx .

In Figures 11 and 12 it was observed that the right-hand portion of each curve became linear where values of θ were greater than 45° . For values of θ less than the angle of repose, NeV^2/Gx does not appear to be affected by changes in θ . A discontinuity exists for values of θ near the flowing angle of repose of the materials. Pictures of flow in the "Discussion of Results" show some evidence of a possible cause of this discontinuity.

The average values of NeV^2/Gx for values of θ indicated are:

$$\text{Milo} - NeV^2/Gx = 0.3388; \theta \leq 30^\circ$$

$$D - NeV^2/Gx = 0.3713; \theta \leq 45^\circ$$

$$B - NeV^2/Gx = 0.4708; \theta \leq 40^\circ$$

Only the linear right-hand portion of the response curve was used in developing component equations. A linear regression analysis was performed for each material. The following component equations were developed.

$$\text{Milo} - NeV^2/Gx = 0.3324 \tan \theta^{1.192} \text{ for } \theta \text{ between } 45^\circ \text{ and } 65^\circ \text{ (6.4)}$$

$$D - NeV^2/Gx = 0.2777 \tan \theta^{0.8229} \text{ for } \theta \text{ between } 45^\circ \text{ and } 65^\circ \text{ (6.5)}$$

$$B - NeV^2/Gx = 0.3466 \tan \theta^{0.9632} \text{ for } \theta \text{ between } 45^\circ \text{ and } 65^\circ \text{ (6.6)}$$

Experiment 5

The angle of friction between the granular material and the wall material, ϕ' , was varied. Four values of ϕ' were used for each material. The means of five replications at each level of ϕ' were plotted in Figure 13.

A linear regression analysis of Gx/NeV^2 on ϕ' was carried out for each material. The slope of the line, or regression coefficient, b , which best fit the observed data was found. The values obtained for "b" and

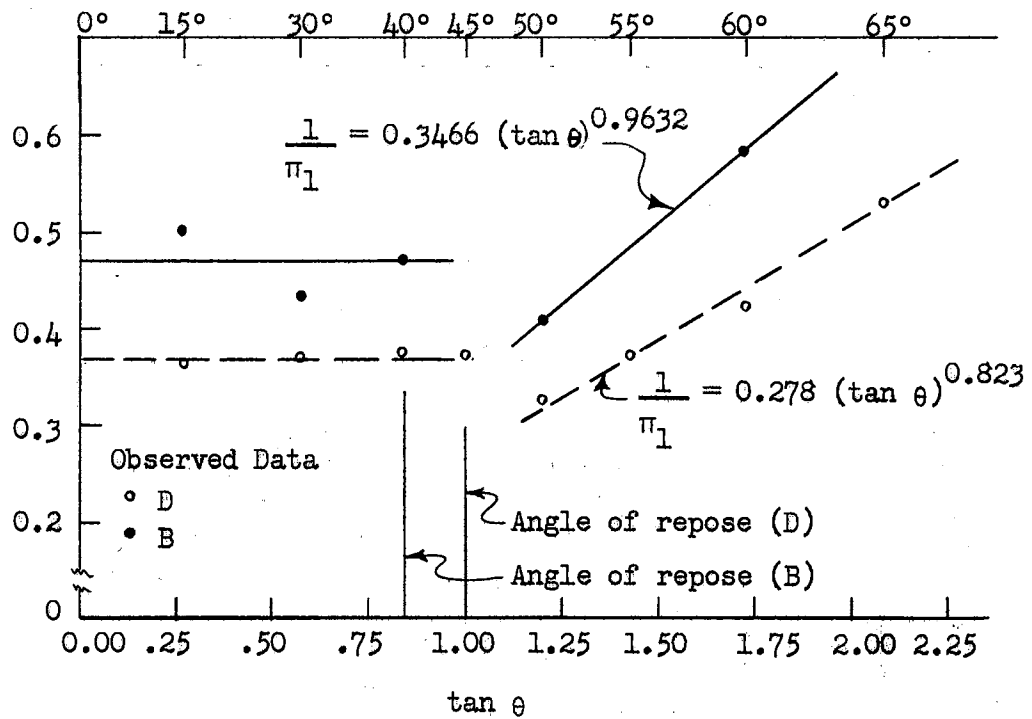


Figure 12. Experiment 4. Effect of Cone Slope θ on $\frac{1}{\pi_1}$ for Materials B and D.

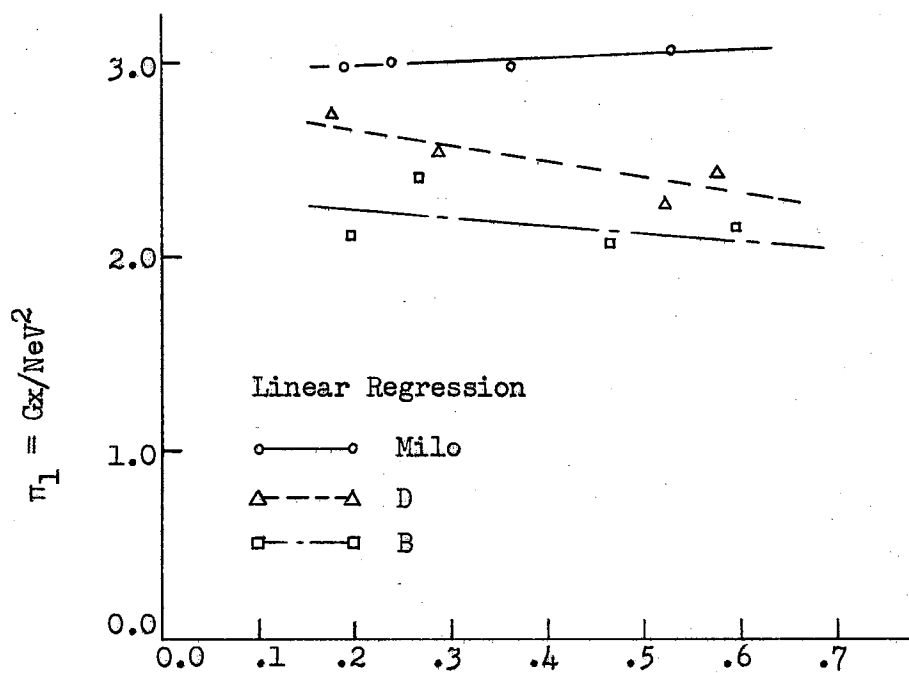


Figure 13. Experiment 5. Effect of ϕ' on $\frac{Gx}{NeV^2}$.

the corresponding correlation coefficients, r , were:

$$b(\text{milo}) = 12.89; \quad b(D) = -44.45; \quad b(B) = -21.80$$

$$r(\text{milo}) = 0.26; \quad r(D) = 0.64; \quad r(B) = 0.58.$$

Statistical "t" tests were performed to determine whether or not the slopes of the regression lines were significantly different from zero: $t = (b - 0.0) / s_b$, where s_b^2 is the variance of the slope, b .

The slope of the regression line for milo was not significantly different from zero at the 90% confidence level. The slopes of the regression lines for materials B and D were significantly different from zero. The accuracy of these tests is not known; since the orifice assembly was not disassembled between replications, the estimate of the error variance does not include assembly error and may be too small.

The product of the slope and the range of $\tan \phi'$ is the predicted difference between the extreme values of Gx/NeV^2 corresponding to the extreme values of $\tan \phi'$. The percent difference predicted is the product divided by the average value of Gx/NeV^2 :

$$b(\tan \phi'_{\text{max.}} - \tan \phi'_{\text{min.}}) / (Gx/NeV^2_{\text{ave.}}) = \text{percent predicted difference.}$$

These values are listed below:

$$\text{Milo} - .2637(0.4065)/2.175 = 4.9\%$$

$$D - .9094(-0.339)/2.498 = -14.0\%$$

$$B - .4460(-0.337)/2.993 = -5.0\%$$

Material D has a relatively large predicted difference as compared to milo and material B. The slope of the regression line for milo was positive and the slopes of the regression lines for materials D and B were negative. There was also a relatively large variation of points

from the regression lines in this experiment as compared to the previous experiments. Since the effects of ϕ' were inconsistent, no component equations were developed and ϕ' was not included in the prediction equation.

Prediction Equations

The general method for combining component equations into one prediction equation is outlined in Murphy, Similitude in Engineering (20). The two basic methods of combination are by addition or multiplication. For combination by multiplication, the component equations should plot as straight lines on logarithmic coordinates. But the component equation for π_4 does not plot as a straight line on logarithmic coordinates. And combination by multiplication would yield a prediction equation which predicts no flow for $\theta = 0^\circ$, which is not true. It was assumed that the component equations could be combined by addition. This method assumes no interaction between the independent variables.

The general prediction equation is of the form,

$$\pi_1 = f_1(\pi_3, \bar{\pi}_4, \bar{\pi}_5, \bar{\pi}_6) + f_2(\bar{\pi}_3, \pi_4, \bar{\pi}_5, \bar{\pi}_6) + \dots + f_n(\bar{\pi}_3, \bar{\pi}_4, \bar{\pi}_5, \pi_6) - (3-2) f_c(\bar{\pi}_3, \bar{\pi}_4, \bar{\pi}_5, \bar{\pi}_6)$$

where $f_n ()$ are component equations and $f_c ()$ is the value of π_1 when all the independent π terms are at their constant values, $\bar{\pi}_i$.

$\pi_2 = H/D$ was deleted earlier in the experiment. Component equations for $\pi_3 = x/d$ and $\pi_6 = \phi'$ were not included since ϕ' did not affect π_1 consistently, and x/d did not affect π_1 for values of x/d greater than 12. The range of values of x/d less than 12 were not considered since most practical applications would be for x/d greater than 12.

The final prediction equations obtained by the above method are:

$$\text{Milo-}\pi_1 = 2.952 \pi_5^{-1.192} - 2.807 \pi_4 + 8.996 \pi_4^2 \quad (6.7)$$

$$\text{D } -\pi_1 = 2.693 \pi_5^{-0.8229} - 1.629 \pi_4 + 11.58 \pi_4^2 \quad (6.8)$$

$$\text{B } -\pi_1 = 2.124 \pi_5^{-0.9632} - 1.448 \pi_4 + 7.300 \pi_4^2 \quad (6.9)$$

CHAPTER VII

DISCUSSION OF RESULTS

Prediction Equations

The component equations developed in Experiments 3 and 4 were combined to yield the following prediction equations.

$$\text{Milo} - Gx/\text{NeV}^2 = 2.952(\tan \theta)^{-1.192} - 2.807 \tan \alpha + 8.996 \tan^2 \alpha$$

$$\text{D} - Gx/\text{NeV}^2 = 2.693(\tan \theta)^{-0.8229} - 1.629 \tan \alpha + 11.58 \tan^2 \alpha$$

$$\text{B} - Gx/\text{NeV}^2 = 2.124(\tan \theta)^{-0.9632} - 1.448 \tan \alpha + 7.300 \tan^2 \alpha$$

These equations are valid only for values of θ greater than 45° and values of x/d greater than 12 due to the limitations of the component equations. The most severe limitation on these equations is that each is valid only for one specific material which has the same physical properties as the material used in this study. However, it is believed that all granular feed materials would yield the same general response as for the three materials used in this study.

It was not possible to compare the experimental data with values of Gx/NeV^2 predicted by the above equations because no data were obtained with x/d greater than 12 and θ greater than 45° at the same time.

The prediction equation above for milo was used to predict values of NeV^2/Gx for typical values of x , θ , and α . These are plotted in Figures 14 and 15.

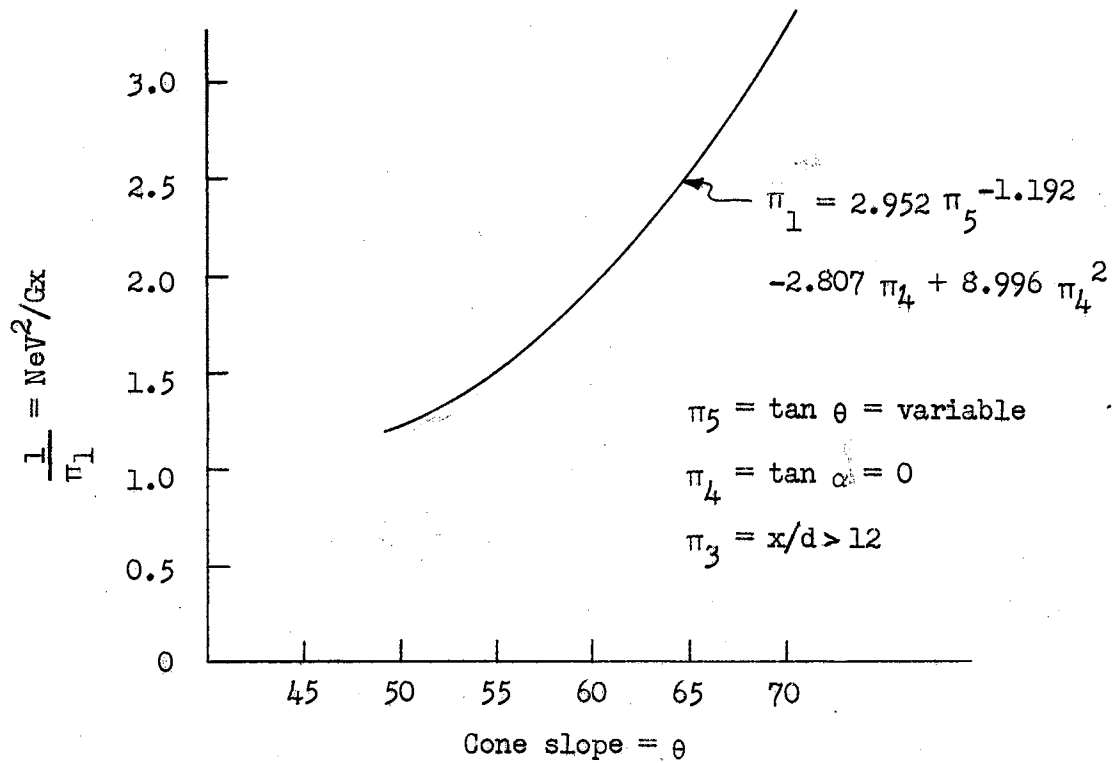


Figure 14. Effect of Cone Slope on NeV^2/Cx Using Prediction Equation for Milo.

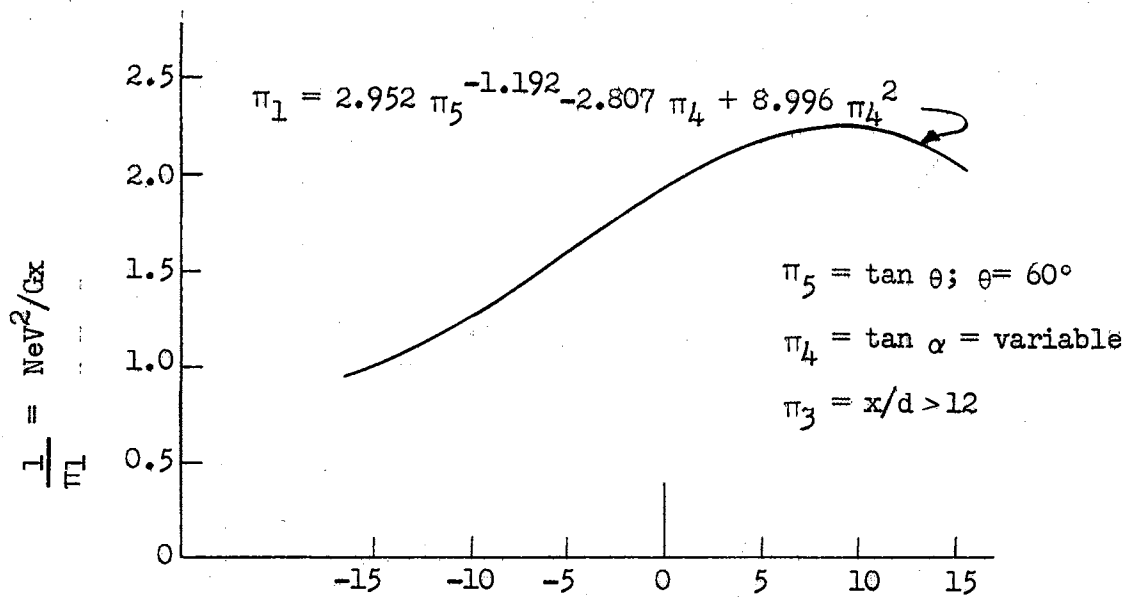


Figure 15. Effect of Outer Wall Slope on NeV^2/Cx using Prediction Equation for Milo.

Comparison of Materials

There were differences in flow velocity among the three materials used. Milo had a higher flow velocity than the ground materials for the larger orifice widths when x/d was greater than 8. The ground materials having smaller particles had higher flow velocities than milo for the narrow orifice widths, since the smaller particles experienced less interference with the orifice. Material D which contained 5% fat and had a higher angle of repose had a 5%-20% lower flow velocity than B which did not contain fat.

In Experiment 4 milo exhibited the slowest flow for cone angles less than or equal to 30° and the fastest flow for cone angles greater than 45° which indicates that milo is more sensitive to changes in cone angles than the materials with a higher shear strength.

Milo had a 2%-12% lower velocity in Experiments 3 and 5 since the cone angle, θ , was less than 45° and x/d (milo) was less than 8.

Figures 16, 17, and 18 show the effect of x , α , and θ , respectively, on flow velocity, V , for all three materials.

Comparison with Previous Research

Several investigators have developed equations relating flow rate to orifice size for circular or polygon-shaped orifices. Some of these equations are listed:

$$V = K(D_o)^{2.93} \quad (\text{Franklin and Johanson})$$

$$V = K(D_o - kd)^{2.5} \quad (\text{Beverloo, Leniger, and van de Velde})$$

$$V = K(A)(d_h)^{0.685} \quad (\text{Fowler and Glastonbury})$$

$$V = K(x)^{2.5} \quad (\text{The present study})$$

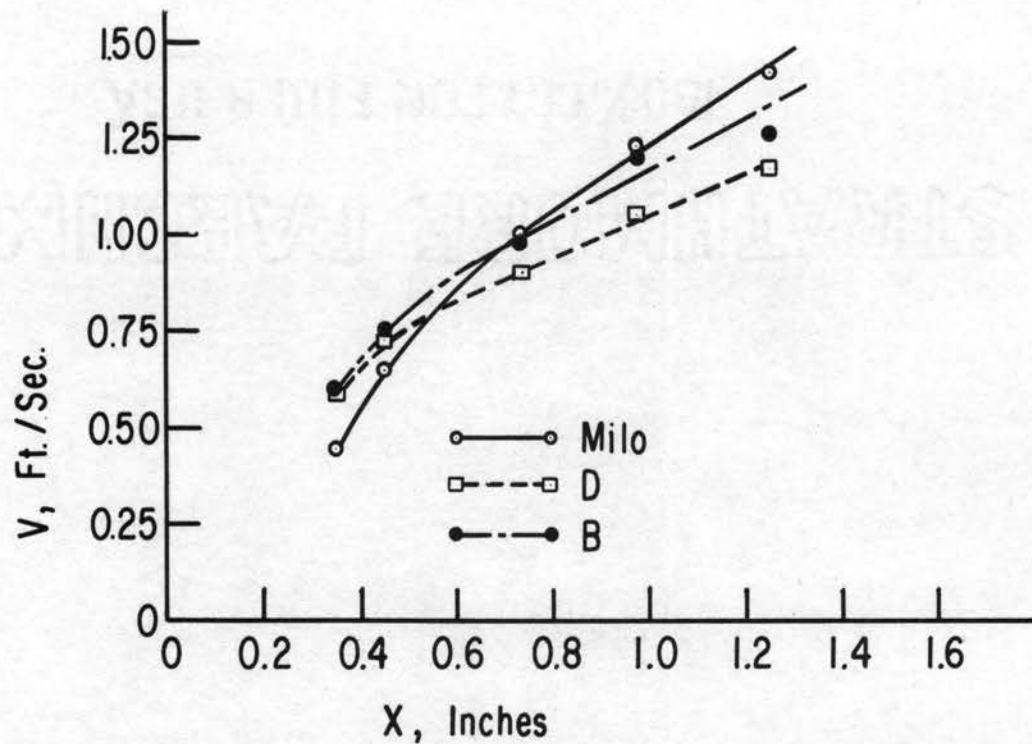


Figure 16. Effect of Orifice Width on Flow Velocity.

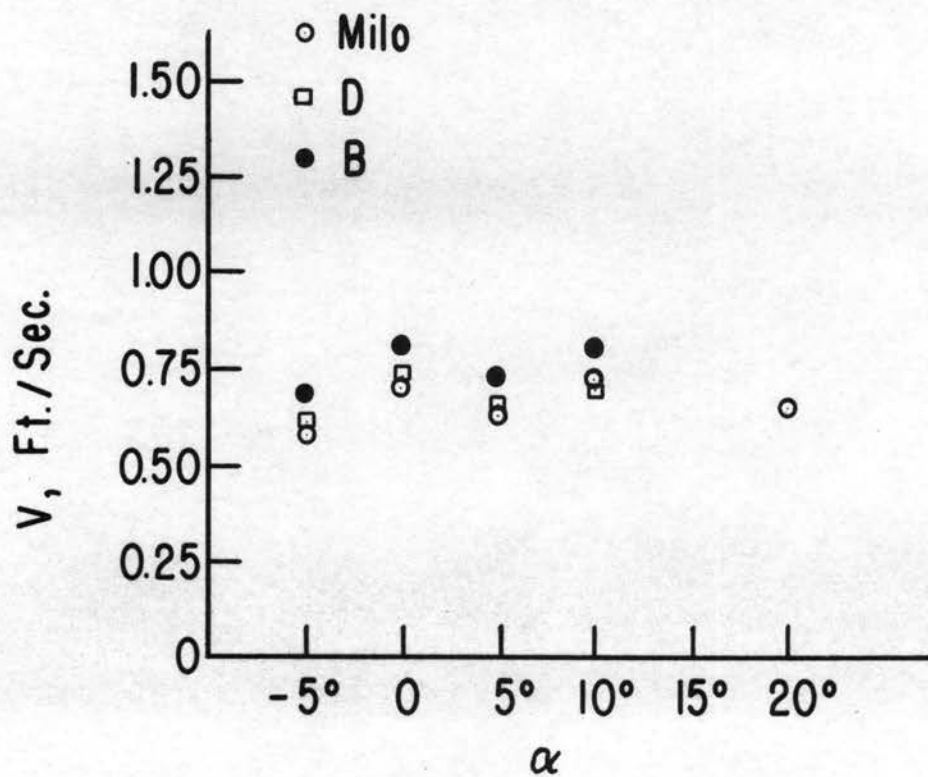


Figure 17. Effect of Outer Wall Slope on Flow Velocity.

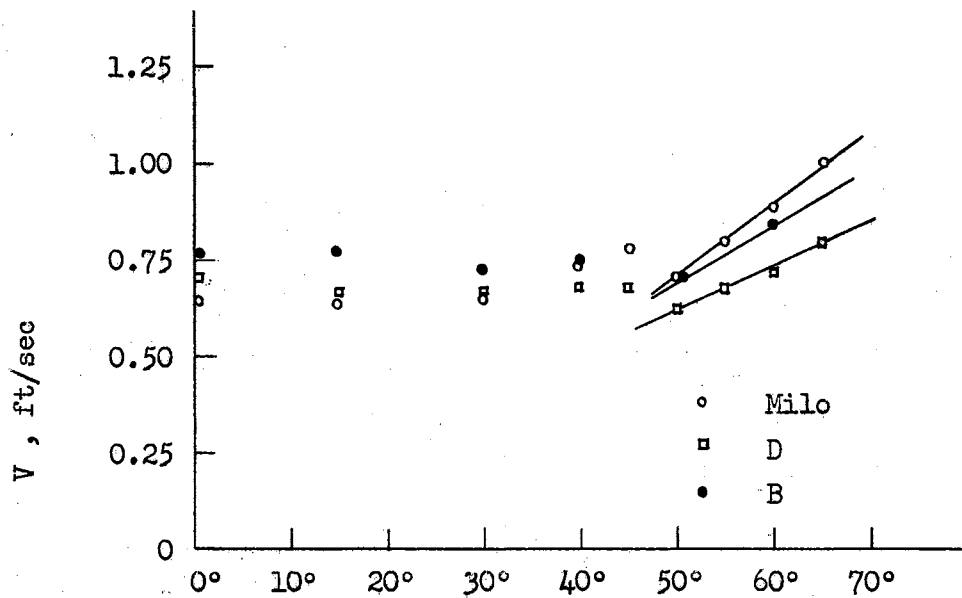


Figure 18. Effect of Cone Slope on Flow Velocity.

D_o is orifice diameter; d_h is hydraulic diameter of orifice; K values are coefficients; d is average particle size; x is annular orifice width; A is orifice area; and V is volume flow rate.

Franklin and Johanson (4) measured flow from cylinders having an orifice in a flat bottom.

Fowler and Glastonbury (7) tested flow of granular materials through circular and polygon-shaped orifices in the bottom of a straight-sided cylinder. The surface roughness of the container was not an important factor. A ratio of orifice width to maximum particle diameter less than 5 affected flow.

Straight-sided cylinders were used by Beverloo, Leniger, and van de Velde (4) to test the flow of seeds through orifices of different sizes and shapes. They found that depths greater than 10 times the orifice diameter produced no effect on flow. The cylinder diameter had no effect. Ratios of orifice diameter to average particle size greater than 20 had a negligible effect on flow.

Flow in Model

Pictures were taken of flow of milo in a glass-sided model with a cross section similar to that of the test hopper. Figures 19, 20, and 21 show the effect of variation in the cone angle θ . The orifice is in the lower right-hand corner of the model. The grid squares are 1 inch by 1 inch.

The pictures were taken using a slow shutter speed of $1/5$ of a second so that the moving seeds were blurred. Figure 19 shows a "cone" angle of 30° which is below the angle of repose for milo. Note that flow occurs only in a vertical section about 5 inches wide. No flow occurs along the "cone" above a depth of 2 inches. Figure 20 shows a "cone" angle of 40° which exceeds the angle of repose for milo. A stationary wall of material still exists about $4\frac{1}{2}$ inches to the left of the vertical wall. In Figure 21 the angle of the cone is 50° . Flow occurs along the entire length of the cone.

It may be noted from Figure 11 that θ has a direct effect on flow velocity only for values of θ greater than 45° . This corresponds with values of θ in the model where flow occurs along the entire lower wall as in Figure 21.

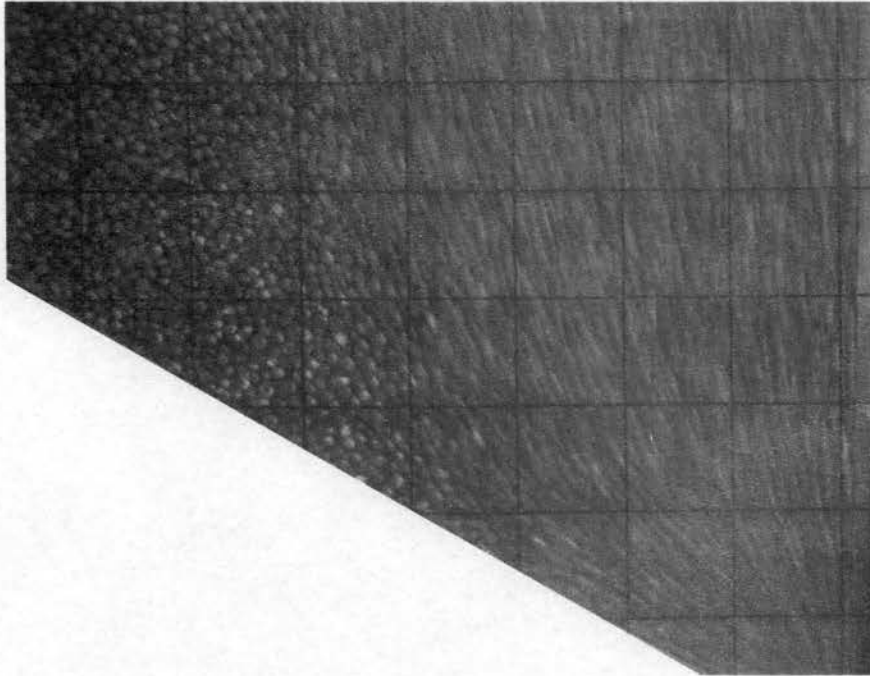


Figure 19. Model Flow, $\alpha = 0^\circ$, $\theta = 30^\circ$.

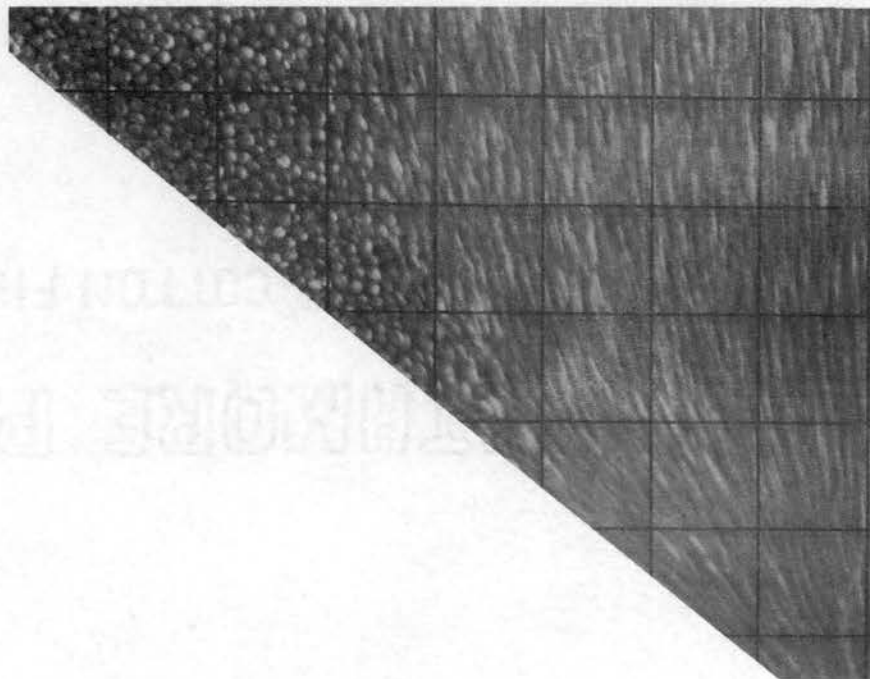


Figure 20. Model Flow, $\alpha = 0^\circ$, $\theta = 40^\circ$.

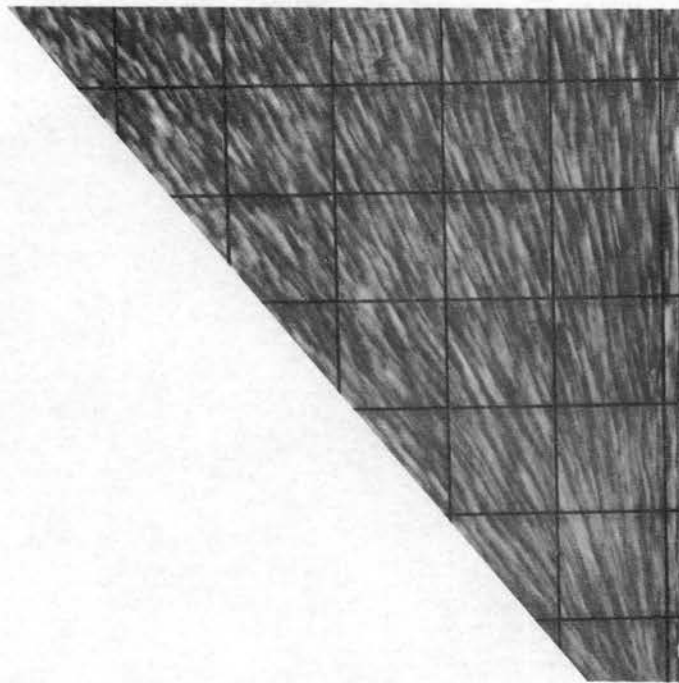


Figure 21. Model Flow, $\alpha = 0^\circ$, $\theta = 50^\circ$.

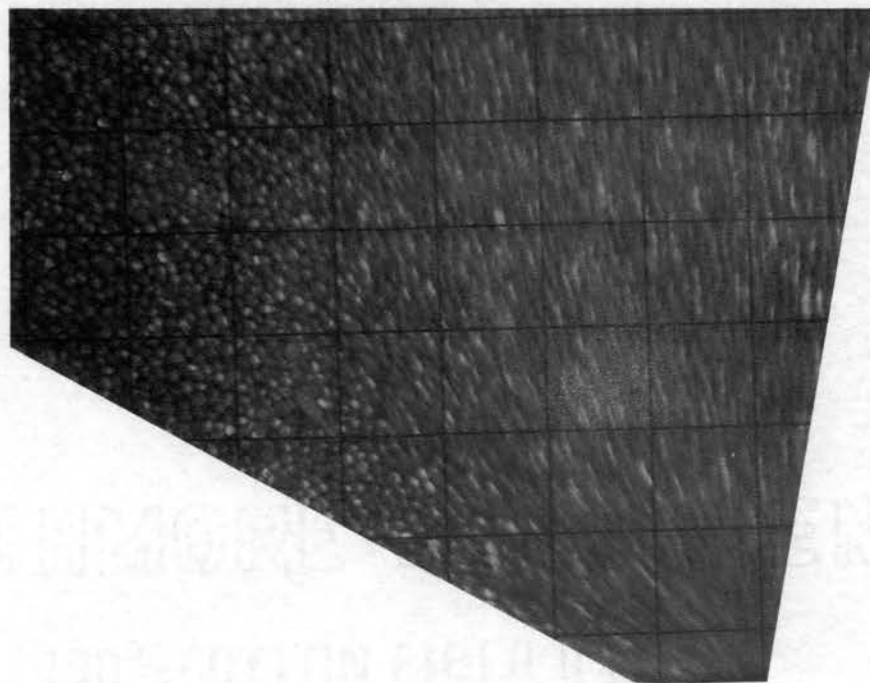


Figure 22. Model Flow, $\alpha = -10^\circ$, $\theta = 30^\circ$.

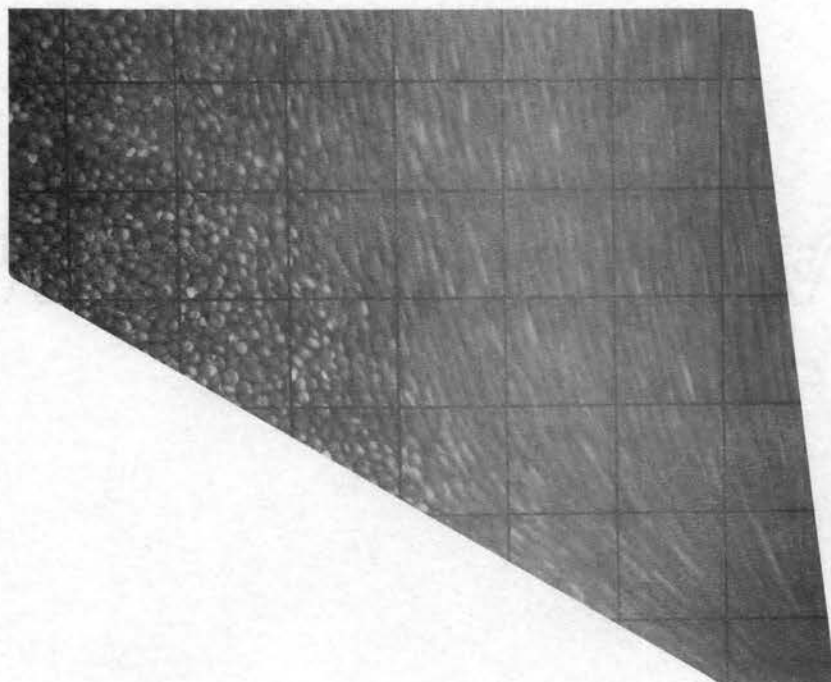


Figure 23. Model Flow, $\alpha = 5^\circ$, $\theta = 30^\circ$.

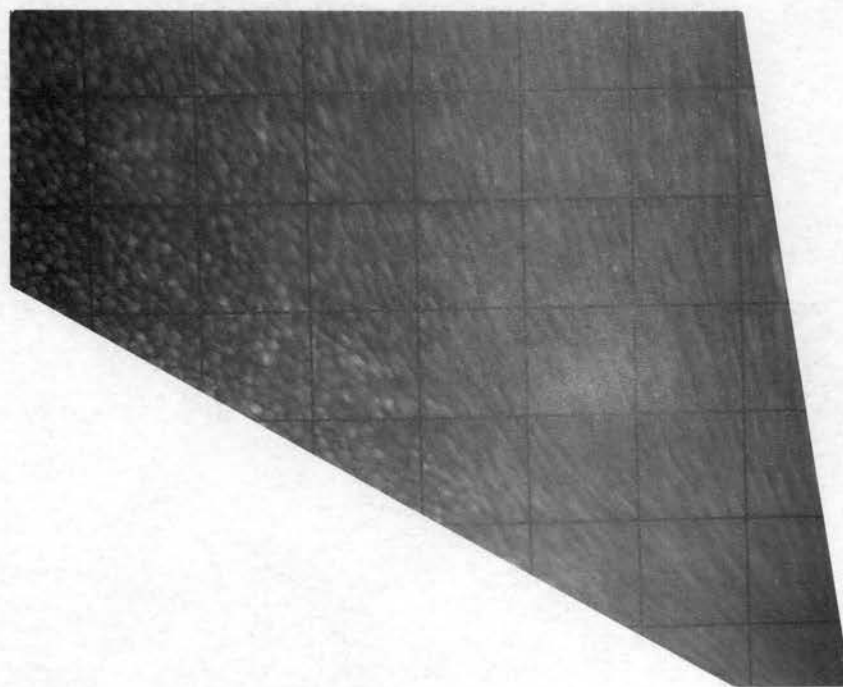


Figure 24. Model Flow, $\alpha = 10^\circ$, $\theta = 30^\circ$.

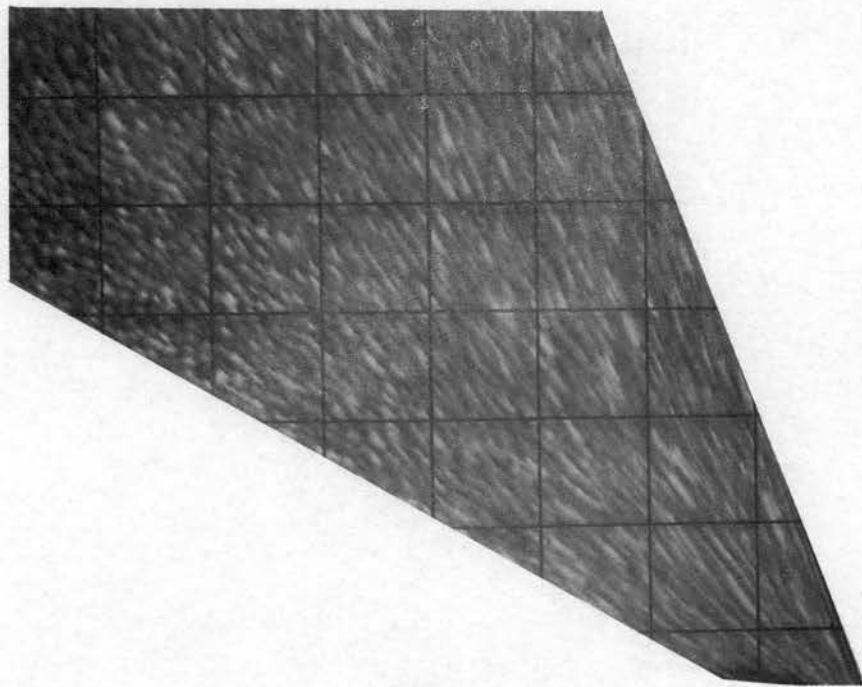


Figure 25. Model Flow, $\alpha = 20^\circ$, $\theta = 30^\circ$.

Figures 22-25 show flow with varying angles of the outer wall, α . Noticeable differences in the flow pattern exist for different values of α . In Figure 25 all particles have a horizontal velocity component due to the slope of the walls. The flow pattern is different in Figure 24 with the flow mostly vertically oriented above a 3 inch depth, since the right wall has a steeper slope. The particles moving along the right-hand wall do not have a horizontal velocity component as large as in Figure 25.

There was a significant difference in Gx/NeV^2 for angles of 0° , 5° , and 10° but Figures 19, 23, and 24 do not reveal any obvious causes of these differences in flow.

Effect of Material Depth

If granular materials behaved like fluids, then the depth of material would affect flow velocity. However, flow of granular materials is not entirely similar to fluid flow since pressure does not increase linearly with depth, and granular materials, unlike fluids, exert static shear forces. The material depth had no effect on flow for depths of the magnitude used in this study, which were greater than 30 times the orifice width.

The lowest depth of material used was 14 inches which was small relative to the size of the test hopper, but large compared to the orifice width. It was believed that the 14 inch depth was still great enough to provide the same density and pressure at the orifice as for greater depths since additional layers of material are supported by the side walls or the cone and may not appreciably increase the density or pressure in the immediate area of the orifice.

It is proposed that the depth of material may still be an important factor where the depth is less than 10 to 30 times the orifice width. In this range of depths, changes in depth would change the bulk density of the mass due to changes in compacting pressures. Jenike (11) showed that increased compacting pressures produced greater shear strength. Higher shear strength would increase resistance to flow.

The flow pattern in a granular material seems to originate at the orifice and develop in an upward direction as the material within the orifice leaves and allows the material directly above it to fall. The mechanics of this particular action occurring within the small area above the orifice would seem to be the controlling factor for orifice flow of granular materials. Then the overall configuration of the container would have much less effect on flow than the portion of the container immediately adjacent to the orifice. This is supported by Laforge and Boruff (16) who propose that the influence of slope and surface roughness is contained in a $3/4$ - 1 inch band immediately adjacent to the orifice.

CHAPTER VIII

SUMMARY AND CONCLUSIONS

An experimental study based on dimensional analysis was conducted to determine the effect of certain factors on gravity flow of granular materials through an annular orifice. Factors studied were orifice width, depth of material, roughness of container walls, and the slopes of the walls adjacent to the orifice. A separate analysis was performed on each of three materials, milo and two ground feed rations.

The bottoms of the test hopper were cones of different heights and the sides were cone frustums or a cylinder. Flow velocity was determined by measuring weight flow rate, converting this to volume flow rate, and dividing by the flow area.

Data was collected varying one dimensionless term at a time. Component equations were developed relating the dependent term, NeV^2/Gx , to each of the independent terms.

From the results of the investigation, the following conclusions concerning flow of granular feed materials through annular orifices are proposed.

1. The system may be described by a general prediction equation of the form: $\pi_1 = C_1 \pi_5^2 + C_2 \pi_4 + C_3 \pi_4^2 + C_4$.

This equation is valid for materials similar to those used in the study where values of x/d are greater than 12 and values of θ are greater than 45° .

2. The depth (H) of material above the orifice is not a pertinent factor affecting flow velocity for values of H greater than 30 times the orifice width.
3. Flow velocity, V, varies as the square root of orifice width, x, for values of x greater than 12 times the average particle diameter. Flow is stopped when x approaches twice the maximum particle size.
4. The roughness of the container walls does not have a marked effect on flow velocity for angles of friction ranging from 10° to 30° . This includes practically all applications having flat walls.
5. The inclination of the container walls immediately adjacent to the orifice is an important factor. This effect is shown graphically in Figures 14 and 15. For the particular configuration used in this study, increases in cone angle above 45° slope increased flow. Flow was constant for slopes less than 45° . Maximum flow velocity occurred when the outer wall sloped inward 5 to 12 degrees from vertical. Changes in wall slope below the angle of repose of the granular material had little effect on flow.
6. The shear strength of the granular material is an important factor. Milo with a lower shear strength than the ground materials had a higher flow velocity except for small orifice widths which obstructed the milo more than the smaller ground particles.

Suggestions for Further Investigations

1. Determine a more precise relationship between flow velocity and slopes of walls adjacent to the orifice using straight rather than cylindrical walls for ease in changing slopes.
2. Develop a general prediction equation for a variety of granular materials. Include one or more measurable physical properties of a granular mass such as shear strength. Vary slopes of walls adjacent to the orifice through a large number of points using slopes greater than 45° .
3. Determine the effect of storage time on flow.
4. Develop a method to predict whether or not a specified granular material will flow in a specific feeder.
5. For non-flowing materials, determine minimum energy requirements for producing flow, and determine feeder configuration for producing flow with minimum energy.

SELECTED BIBLIOGRAPHY

1. Balis, J. S. "Methodology on the Determination of Friction Coefficients of Agricultural Materials." Purdue University Engineering Experiment Station Research Service. 140:26-27. 1959.
2. Barre, H. J. "Flow of Bulk Granular Materials." Agricultural Engineering 39:9:534-536. September, 1958.
3. Barre, H. J. and L. L. Sammet. Farm Structures. New York: John Wiley and Sons, Inc. p. 629. 1950.
4. Beverloo, W. A., H. A. Leniger, and J. van de Velde. "The Flow of Granular Solids Through Orifices." Chemical Engineering Science. 15:260-269. 1961.
5. Brown, R. L. and P. G. Hawksley. "The Internal Flow of Granular Masses." Fuel. 26:6:161. 1947.
6. Carmody, R. "Hot Feed." Farm Quarterly. 16:90-5. 1961.
7. Endersby, V. A. "The Mechanics of Granular and Granular-Plastic Materials, With Special Reference to Bituminous Road Materials and Subsoils." American Society for Testing Materials. 40:1155-1172. 1940.
8. Fowler, R. T. and J. R. Glastonbury. "The Flow of Granular Solids Through Orifices." Chemical Engineering Science. 10:150-156. 1959.
9. Fowler, R. T. and W. B. Chodziesner. "The Influence of Variables Upon the Angle of Friction of Granular Materials." Chemical Engineering Science 10:157-162. 1959.
10. Freer, M. "Factors Affecting Voluntary Intake of Food by Cows." British Journal of Nutrition. 16:279. 1962.
11. Jenike, Andrew W. "Better Design for Bulk Handling." Chemical Engineering. 61:12:175. December, 1954.
12. Jenike, Andrew W. "Gravity Flow of Bulk Solids." Utah Engineering Experiment Station. 52:215-241. 1961.
13. Johanson, J. R. and Jenike, A. W. "Stress and Velocity Fields in Gravity Flow of Bulk Solids." Utah Engineering Experiment Station. 53:21. 1962.

14. Kondner, Robert L. and Gordon E. Green. "Stress Distribution in Earth Masses." Highway Research Bulletin 342. 1962.
15. Kondner, Robert L. and Raymond Krizek. "Correlation of Load Bearing Tests on Soils." Highway Research Board; Proceedings. 41:560-562. 1962.
16. Laforge, Robert M. and Billy K. Boruff. "Profiling Flow of Particles Through Hopper Openings." Industrial and Engineering Chemistry. 56:2:42-46. February, 1964.
17. Lee, Chesman A. "Hoppers by Calculation?" Chemical Engineering. 61:12:181. December, 1954.
18. Loosli, J. K. "Frequent Feeding Can Increase Performance." Hoard's Dairyman. 105:1198. December, 1960.
19. _____ . "Method of Determining Modulus of Uniformity and Modulus of Fineness of Ground Feed." Agricultural Engineers Yearbook. American Society of Agricultural Engineers. 1964.
20. Mochrie, R. D. "Influence of Frequency of Feeding Equalized Intakes on Animal Response." Journal of Animal Science. 15:1256. 1956.
21. Mohrman, R. K. "The Influence of Hand-feeding, Self-feeding, and Frequent-Interval-Feeding on Performance and Behavior of Beef Cattle." Journal of Animal Science. 18:1489. 1959.
22. Morrison, F. B. Feeds and Feeding. New York: Morrison Publishing Co. p. 76. 1948.
23. Murphy, Glenn. Similitude in Engineering. New York: The Roland Press Company. 1950.
24. Putnam, P. A. and R. E. Davis. "Ration Effects on Drylot Steer Feeding Patterns." Journal of Animal Science. 21:1009. 1962.
25. Raun, Ned. "Fine Sand, Frequent Feeding Show Prospect of Faster Gains in Cattle." Breeder's Gazette. 126:18. August, 1961.
26. Singley, Mark E. "Handling Non-Free-Flowing Materials." Agricultural Engineering. 39:9:540-542. September, 1958.
27. Swift, R. W. "The Nutritive Evaluation of Forages." Pennsylvania Agricultural Experiment Station Bulletin 615. 1957.

APPENDIX A
SYMBOLS AND NOTATION

SYMBOLS AND NOTATION

b	Slope of Regression Line
d	Average Particle Diameter
D	Bottom Diameter of Cone
E	Modulus of Elasticity
F	Dimensional Symbol for Force
G	Gravitational Field Strength
H	Depth of Material Above Orifice
L	Dimensional Symbol for Length
M	Dimensional Symbol for Mass
Ne	Newton's Second Law Coefficient
r	Correlation Coefficient
t	Thickness of Walls
T	Dimensional Symbol for Time
V	Instantaneous Flow Velocity
x	Width of Orifice
α	Slope of Outer Wall
θ	Slope of Cone
π	Dimensionless Term
ρ_B	Bulk Mass Density
v	Voids Ratio of Granular Material
ϕ	Internal Angle of Friction of Material
ϕ'	Angle of Friction Between Granular Material and Metal Surfaces

APPENDIX B
EXPERIMENTAL DATA

The values of the pi terms for each experiment are listed in the following tables.

The value of G/Ne was constant at 32.2 ft/sec.^2 for each experiment. D remained constant at 18.05 inches. The value of "d" was constant for each material throughout all of the experiments: $d(\text{milo}) = 0.127 \text{ in.}$; $d(D) = 0.048 \text{ in.}$; and $d(b) = 0.041 \text{ in.}$

"H" and "x" were held constant at 22 in. and 0.450 in., respectively, for experiments 3, 4, and 5.

EXPERIMENT 1.

Variable level	$\pi_2 = \frac{H}{D}$	Replication	$\pi_1 = \frac{GH}{NeV^2}$		
			Milo	D	B
a	0.775	1	39.79	47.92	38.02
		2	38.41	50.30	40.11
		3	39.92	47.80	49.29
		4	38.24	46.51	52.72
		5	39.47	47.38	41.29
b	0.996	1	52.34	61.76	54.81
		2	50.57	60.39	50.69
		3	53.15	64.09	51.96
		4	49.78	61.76	52.72
		5	53.90	65.09	52.05
c	1.217	1	61.81	79.25	64.35
		2	64.73	74.10	66.74
		3	63.10	80.18	61.96
		4	60.16	81.65	68.43
		5	58.68	81.87	65.49
d	1.439	1	73.23	83.46	80.01
		2	74.39	88.12	79.53
		3	73.89	91.16	78.59
		4	69.63	93.16	78.13
		5	74.75	90.23	79.72
e	1.660	1	83.15	105.4	89.93
		2	80.58	96.16	92.87
		3	84.49	101.0	93.10
		4	83.71	104.0	90.04
		5	83.61	108.2	92.64
f	1.882	1	101.4	115.4	103.8
		2	105.1	119.8	110.5
		3	97.85	116.1	101.3
		4	100.9	117.9	110.0
		5	100.3	119.7	104.6

	Milo	D	B
x/d	5.791	-15.312	-17.927
tan α	0.000	0.000	0.000
tan θ	0.5774	0.5774	0.5774
tan ϕ	0.1994	0.1763	0.1944

EXPERIMENT 2

Variable level	x/d			Repli- cation	Gx/NeV ²		
	Milo	D	B		Milo	D	B
a	2.756	7.292	8.537	1	4.517	2.740	2.833
				2	4.496	2.935	2.890
				3	4.722	2.447	2.378
				4	5.453	2.763	2.674
				5	4.917	2.664	2.413
b	3.543	9.375	10.976	1	2.655	2.320	2.493
				2	2.996	2.053	1.980
				3	2.898	2.306	1.932
				4	2.891	2.278	2.069
				5	2.774	2.302	2.030
c	5.791	15.312	17.927	1	1.745	2.408	2.106
				2	2.030	2.525	1.775
				3	1.926	2.328	2.047
				4	2.014	2.404	1.996
				5	2.021	2.363	2.086
d	7.677	20.313	23.780	1	1.647	2.323	1.908
				2	1.718	2.323	1.918
				3	1.741	2.342	1.841
				4	1.754	2.299	1.693
				5	1.772	2.342	1.835
e	9.803	25.938	30.366	1	1.569	2.226	2.065
				2	1.616	2.383	2.054
				3	1.655	2.548	2.117
				4	1.673	2.395	2.256
				5	1.705	2.677	2.048

$\tan \alpha = 0.000$; $\tan \theta = 0.5774$; $\tan \phi'$ (milo) = 0.1944; $\tan \phi'$ (D) = 0.1780; $\tan \phi'$ (B) = 0.1944

EXPERIMENT 3

Variable level	$\pi_4 = \tan \alpha$	Repli- cation	$\pi_1 = Gx/NeV^2$		
			Milo	D	B
a	-0.1763	1	3.626	3.349	2.821
		2	3.795	2.942	2.451
		3	3.511	3.079	2.551
		4	3.464	3.124	2.453
		5	3.460	3.409	2.551
b	0.0000	1	2.502	2.361	1.759
		2	2.429	2.312	1.788
		3	2.431	2.156	1.861
		4	2.394	2.261	1.919
		5	2.449	2.212	1.908
c	0.0875	1	3.034	2.860	2.146
		2	3.100	2.758	2.418
		3	3.010	2.674	2.234
		4	3.040	2.660	2.279
		5	3.104	2.807	2.165
d	0.1763	1	2.349	2.515	1.834
		2	2.392	2.508	2.006
		3	2.320	2.517	1.916
		4	2.296	2.339	1.852
		5	2.197	2.382	2.000
e	0.3640	1	2.830		
		2	2.727		
		3	2.885		
		4	3.139		
		5	3.114		

	Milo	D	B
x/d	3.543	9.375	10.976
$\tan \theta$	0.5774	0.5774	0.5774
$\tan \phi'$	0.2680	0.2680	0.2680

EXPERIMENT 4

Variable level	$\pi_5 = \tan \theta$	Repli- cation	$\pi_1 = Gx/NeV^2$		
			Milo	D	B
a	0.0000	1	2.942	2.283	2.240
		2	2.965	2.564	1.949
		3	2.997	2.482	1.944
		4	2.959	2.355	2.045
		5	2.995	2.537	2.048
b	0.2679	1	2.932	2.641	1.850
		2	2.897	2.723	1.913
		3	3.018	2.623	2.095
		4	3.085	2.776	2.066
		5	3.022	2.895	2.120
c	0.5774	1	2.664	2.793	2.594
		2	2.838	2.658	2.289
		3	3.137	2.729	2.199
		4	2.901	2.742	2.214
		5	2.952	2.699	2.222
d	0.8391	1	2.234	2.625	2.105
		2	2.206	2.866	2.111
		3	2.214	2.580	2.031
		4	2.228	2.682	2.132
		5	2.187	2.541	2.193
e	1.0000	1	1.992	2.658	
		2	2.001	2.611	
		3	1.949	2.670	
		4	1.996	2.641	
		5	2.040	2.709	
f	1.1918	1	2.422	3.061	2.656
		2	2.365	3.038	2.478
		3	2.498	3.004	2.353
		4	2.390	3.065	2.347
		5	2.490	3.114	2.412
g	1.4281	1	1.991	2.676	
		2	1.995	2.674	
		3	2.073	2.727	
		4	1.938	2.607	
		5	1.855	2.727	
h	1.7321	1	1.622	2.379	1.808
		2	1.619	2.418	1.663
		3	1.586	2.455	1.569
		4	1.539	2.281	1.724
		5	1.489	2.281	1.719
i	2.1445	1	1.218	1.594	
		2	1.216	1.846	
		3	1.182	1.893	
		4	1.216	2.022	
		5	1.201	2.125	

EXPERIMENT 4 (CONT'D)

	Milo	D	B
x/d	3.543	9.375	10.976
$\tan \phi'$	0.1944	0.1763	0.1944
$\tan \alpha$	0.0000	0.0000	0.0000

EXPERIMENT 5

Variable level	$\pi_0 = \tan \phi'$			Repli- cation	$\pi_1 = Gx/NeV^2$		
	Milo	D	B		Milo	D	B
a	0.1944	0.1763	0.1944	1	2.887	2.848	2.060
				2	2.975	2.576	1.975
				3	2.928	2.711	2.107
				4	2.948	2.770	2.126
				5	2.952	2.752	2.263
b	0.2309	0.2868	0.2680	1	2.756	2.993	2.572
				2	3.036	2.754	2.404
				3	3.126	2.429	2.294
				4	2.985	2.488	2.398
				5	2.993	2.326	2.390
c	0.3640	0.5095	0.4663	1	2.838	2.244	2.097
				2	2.959	2.234	2.058
				3	2.952	2.281	2.114
				4	3.032	2.238	2.045
				5	2.916	2.292	1.936
c	0.5317	0.5774	0.6009	1	3.075	2.588	2.171
				2	3.116	2.506	2.069
				3	3.112	2.459	2.091
				4	3.110	2.101	2.175
				5	3.153	2.549	2.154

	Milo	D	B
x/d	3.543	9.375	10.976
tan α	0.000	0.000	0.000
tan θ	0.5774	0.5774	0.5774

VITA

VINCENT E. SWEAT

Candidate for the degree of

Master of Science

Thesis: AN EXPERIMENTAL ANALYSIS OF GRAVITY-INDUCED FLOW OF
GRANULAR MATERIALS THROUGH AN ANNULAR ORIFICE

Major Field: Agricultural Engineering

Biographical:

Personal Data: Born at Kirwin, Kansas, July 28, 1941, the
son of Eugene and Jean Sweat.

Education: Graduated from Kensington High School, Kensington,
Kansas, in 1959. Received the Bachelor of Science degree
in Agricultural Engineering in January, 1964, from Kansas
State University; completed the requirements for the
Master of Science degree in May, 1965.

Experience: Served as a graduate research assistant for the
Agricultural Engineering Department, Oklahoma State Univer-
sity, for one year.

Associate Member of American Society of Agricultural Engineers.